

Data Descriptor

Removal of Positive Elevation Bias of Digital Elevation Models for Sea-Level Rise Planning

Elizabeth Burke Watson ^{1,*}, LeeAnn Haaf ², Kirk Raper ³ and Erin Reilly ^{4,5}

¹ Department of Biodiversity, Earth & Environmental Sciences and the Academy of Natural Sciences, Drexel University, Philadelphia, PA 19103, USA

² Partnership for the Delaware Estuary, Wilmington, DE 19801, USA; lhaaf@delawareestuary.org

³ Academy of Natural Sciences, Drexel University, Philadelphia, PA 19103, USA; klr323@drexel.edu

⁴ The Barnegat Bay Partnership, Toms River, NJ 08754, USA; ereilly@umces.edu

⁵ University of Maryland Center for Environmental Science, MD 20688, USA

* Correspondence: elizabeth.b.watson@gmail.com; Tel.: +01-215-299-1109

Received: 7 March 2019; Accepted: 21 March 2019; Published: 26 March 2019



Abstract: Digital elevation models (DEMs) based on LiDAR surveys provide critical information for predicting the vulnerability of coastal areas to sea-level rises. Due to the poor penetration of LiDAR pulses in marsh vegetation, bare-earth DEMs for coastal wetlands are often subject to positive elevation bias, and thus underestimate vulnerability. This data publication includes comprehensive elevation surveys from seven coastal wetlands in coastal New Jersey, and an evaluation of the accuracy and positive elevation bias of each publically available DEM. Resampling the DEMs at a coarser resolution, replacing cell values using the minimum value in a wider search window (4 m), removed this positive elevation bias with no loss of accuracy.

Dataset: The following are available online at <http://www.mdpi.com/2306-5729/4/1/46/s1>.

Dataset License: CC0

Keywords: LiDAR; post-processing; coastal marsh; signed error

1. Summary

The rate of global sea-level rise (SLR) has increased abruptly, relative to stable Late Holocene rates of 0.5–1.0 mm yr⁻¹ that have prevailed over the last 2000 years [1,2], to 1.7 ± 0.3 mm·yr⁻¹ during the 20th century [3] and 3.1 ± 0.3 mm yr⁻¹ since 1993 [4]. These rates of SLR are associated with trends in increasing temperature [5,6], and studies have generally concluded that statistically significant SLR acceleration is occurring [4]. Although there is significant variability by region in projected SLR rates, global rates by 2100 predicted by the IPCC AR5 report ranged from 28–61 to 52–98 cm, depending on emission scenarios. SLR will impact millions of coastal residents over the coming decades [7] and there is a strong need for accurate elevation models to characterize vulnerability to SLR for both the built environment, as well as coastal habitats such as dunes, beaches, and wetlands, which can act as natural defenses against SLR.

Coastal wetlands can protect coastal communities from event-based flooding, which is amplified by SLR [8]. However, they are themselves quite vulnerable to climate change, as their sustainability depends on the interplay between organic soil formation and sediment deposition relative to SLR rates [9]. If marshes can build up faster than the sea rises, they will be sustainable. If SLR exceeds accumulation rates, marshes will drown, and in this context, millimeters matter [9]. Although digital elevation models derived from light detection and ranging (LiDAR) surveys can be as accurate as

typical GPS ground surveys (± 5 cm), the presence of thick vegetation in coastal wetlands obstructs the ground surface, leading to positive elevation biases that can result in underestimations of climate change vulnerability [10].

This dataset includes elevation data surveys (~3200 points) from seven New Jersey coastal wetlands, and was collected to ascertain the level of positive elevation bias found in digital elevation models (DEMs). We found that positive elevation biases (measured as signed error) ranged up to 0.3 m, which could significantly affect assessments of wetland vulnerability to SLR (Table 1). Post-processing DEMs using a minimum bin method largely removed positive elevation biases with minimal losses in accuracy (Figure 1). We found that resampling the DEM at 4 m resolution using the minimum bin method resulted in no loss of accuracy as measured by root mean square error (RMSE), but reduced the signed error from an average of 12 to 1.5 cm. Resampling at 5 m resolution increased the RMSE from 21 to 23 cm, and shifted the signed error to a negative elevation bias of -1.0 cm.

Table 1. Vertical elevation differences for the as-received LiDAR vs. topographic surveys.

Site Name	DEM ¹	No. of Points	RMSE (cm)	Signed Error (cm)	25th Quartile (cm)	75th Quartile (cm)
Crosswicks Creek	2015 USGS	572	22.1	-4.59	-14.4	-1.3
Dividing Creek	2015 USGS	875	27.3	13.9	2.62	19.6
Maurice River	2015 USGS	162	19.4	16.8	11.0	22.7
Dennis Creek	2014 NOAA	223	27.0	24.8	17.4	30.3
Dennis Creek	2015 USGS	223	35.7	28.6	16.7	35.8
Reedy Creek	2014 NOAA	329	11.7	8.79	3.75	13.2
Reedy Creek	2015 USGS	329	12.5	7.48	2.03	10.1
Island Beach	2013 USACE	294	13.9	9.35	1.55	14.7
Island Beach	2014 NOAA	294	9.87	7.40	2.91	10.6
Island Beach	2015 USGS	294	14.9	7.18	1.62	8.33
Channel Creek	2010 ARRA	697	22.7	11.4	1.38	10.9
Channel Creek	2013 USACE	697	31.2	24.0	12.3	26.3
Channel Creek	2014 NOAA	697	20.9	10.4	4.34	14.9
Channel Creek	2015 USGS	697	25.8	5.90	-1.36	7.60

¹ See Table 3 and metadata for full explanation of digital elevation models (DEMs).

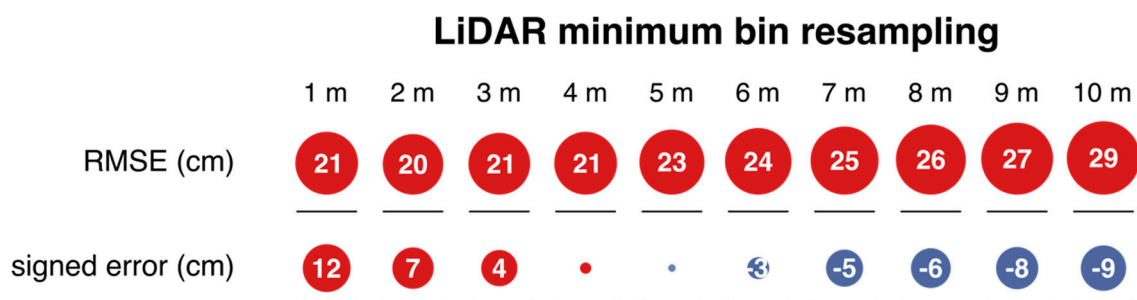


Figure 1. Comparison of RMSE and signed error for DEMs resampled using the minimum bin method.

However, several of the DEMs we worked with did not conform to this trend and maintained a positive elevation bias even after post-processing (Figure 2), such as the 2013 DEM covering the research site at Channel Creek and the 2015 DEM covering Dennis Creek. In such cases, it may be more beneficial to use masks, potentially based on plant cover class, to improve DEM accuracy. This method has been used widely in coastal wetlands outside the Northeastern U.S., where the plant cover is found throughout the year (e.g., [11]). In the Northeast, by collecting LiDAR data in spring leaf-off conditions when the vegetation cover is sparse, the need for masks has largely been avoided.

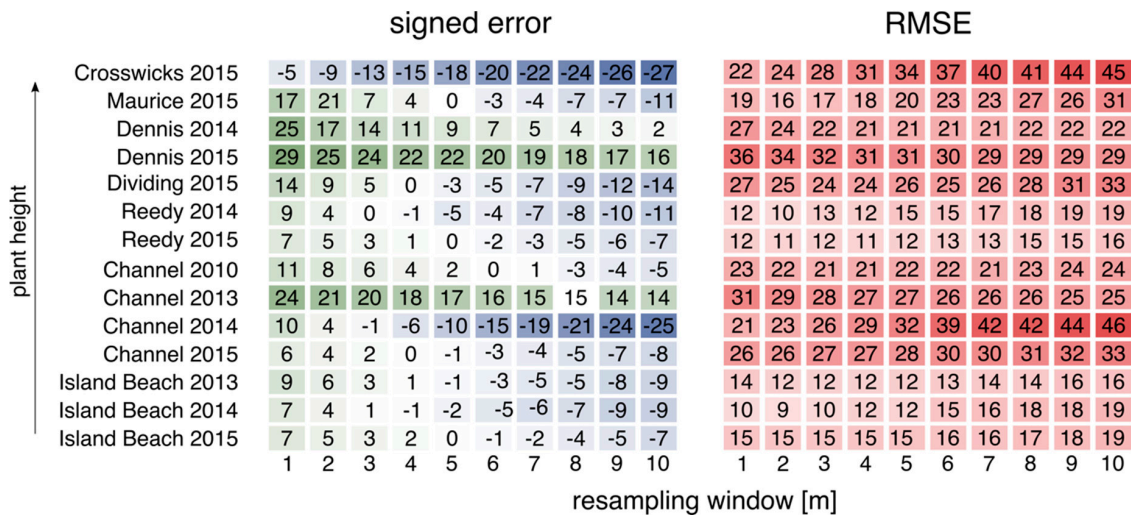


Figure 2. Comparison of RMSE and signed error for resampled DEMs (in cm).

By publishing this dataset, we intend for it to be used to guide DEM post-processing and to develop new DEM post-processing methods relevant to predicting impacts of sea-level rise in vegetated coastal areas. Future work using this data will include validating and applying SLR models for predicting coastal wetland vulnerability to climate change.

2. Data Description

2.1. Elevation Survey Points

Shapefiles of surveyed elevation points are provided for each individual study site (Table 2). These shapefiles consist of an elevation field, where the elevations are given in meters relative to the NAVD88 datum, GEOID12A. Elevation surveys were conducted between 2014 and 2018. A data inventory is provided (Supplementary Material, File 1).

Table 2. Surveyed locations in New Jersey coastal wetlands (Supplementary Material, File 2).

Site Name	Location	Salinity	Vegetation Height (m)
Crosswicks Creek	40°9.76' N, 74°42.51' W	0.10‰	1.2 m
Dividing Creek	39°14.14' N, 75°6.76' W	16.7‰	0.32 m
Maurice River	39°15.95' N, 74°59.72' W	11.2‰	0.56 m
Dennis Creek	39°10.58' N, 74°51.74' W	15.9‰	0.34 m
Reedy Creek	40°1.74' N, 74°5.07' W	20.2‰	0.29 m
Island Beach	39°47.96' N, 74°6.10' W	26.8‰	0.17 m
Channel Creek	39°37.43' N, 74°16.20' W	25.6‰	0.23 m

2.2. Digital Elevation Model Metadata

Metadata is provided for the publically available DEMs analyzed as part of this study (Supplementary Material, File 3), following the Content Standard for Digital Geospatial Metadata: Extensions for Remote Sensing Metadata, FGDC-STD-012-2002. For each site, all publically available DEMs were analyzed, which ranged from one to four DEMs per study site (Table 3). For all DEMs, the initial resolution was 1 m, although DEMs were resampled and analyzed at a coarser resolution. A data inventory is provided (Supplementary Material). The 2010 DEM was adjusted from the GEOID09 to GEOID12A. The 2015 United State Geological Survey (USGS) topobathy DEM covers all of New Jersey and Delaware coastal areas, and consists of the best available multi-source topographic and bathymetric elevation data, integrating over 89 different data sources, including topographic and

bathymetric LiDAR point clouds, hydrographic surveys, side-scan sonar surveys, and multi-beam surveys from various federal, state, and local agencies.

Table 3. Topobathy DEMs analyzed by this study.

Site Name	Digital Elevation Model	Resolution	Date	Sensor
Crosswicks	2015 USGS CoNED	1 m	multiple years	multiple sensors
Dividing	2015 USGS CoNED	1 m	multiple years	multiple sensors
Maurice	2015 USGS CoNED	1 m	multiple years	multiple sensors
Dennis	2014 NOAA Post-Sandy	1 m	Nov 2013–June 2014	Riegl VQ-820G
Dennis	2015 USGS CoNED	1 m	multiple years	multiple sensors
Reedy	2014 NOAA Post-Sandy	1 m	Nov 2013–June 2014	Riegl VQ-820G
Reedy	2015 USGS CoNED	1 m	multiple years	multiple sensors
Island Beach	2013 USACE NCMP	1 m	Sept 2013–Oct 2013	CZMIL (USACE)
Island Beach	2014 NOAA Post-Sandy	1 m	Nov 2013–June 2014	Riegl VQ-820G
Island Beach	2015 USGS CoNED	1 m	multiple years	multiple sensors
Channel	2010 ARRA	1 m	Apr 2010	Leica ALS60 MPiA
Channel	2013 USACE NCMP	1 m	June 2013	CZMIL (USACE)
Channel	2014 NOAA Post-Sandy	1 m	Nov 2013–June 2014	Riegl VQ-820G
Channel	2015 USGS CoNED	1 m	multiple years	multiple sensors

3. Methods

Elevation surveys were conducted in seven separate New Jersey (USA) coastal wetlands at long-term monitoring locations (<https://www.macwa.org>), using real-time kinematic GPS receivers (a Leica Viva GS14 GNSS Receiver and Viva CS15 field controller, or a Trimble R6 GNSS receiver and TSC2 data controller) to assess the vertical accuracy of bare-earth DEMs based on LiDAR surveys. Data collection followed National Geodetic Survey guidelines for the RT3 accuracy class (0.04–0.06m horizontal precision; 0.04–0.08 vertical precision): Baselines < 20 km and collection at 1 s intervals for 15 s, with a steady fixed height rover pole without use of a tripod [12]. Study sites were located in Barnegat Bay and Delaware Bay, New Jersey, USA (Table 2; Figure 3). Mean vegetation height and salinity were found to vary quite widely across study sites [13], with strong co-variance between salinity and the height of marsh vegetation, with lower salinity wetlands supporting taller marsh vegetation ($r^2 = 0.89$, $p = 0.001$). Elevation surveys were conducted between 2014 and 2018. Surveyed points were downloaded from data controllers, and converted to point shapefiles (Supplementary Materials, File 2).

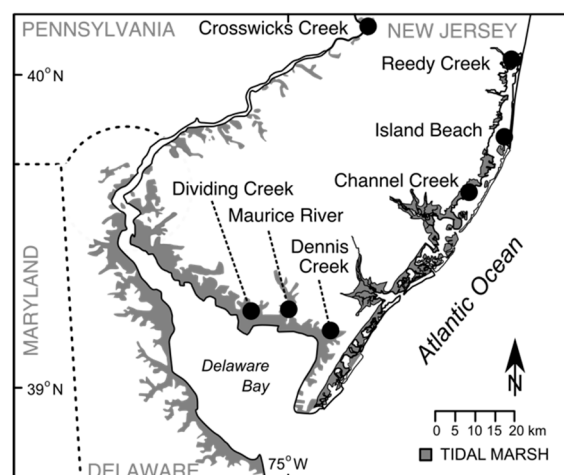


Figure 3. Location of elevation surveys and LiDAR comparisons.

All publicly available DEMs available for research sites were obtained (Table 3). To assess differences in elevation between the two datasets, points were intersected with as-delivered DEMs, as well as DEMs post-processed using the minimum bin method [14]. The minimum bin technique

selects the lowest point in a cell to represent the grid or raster value, increasing the search window from two to ten meters. DEMs were then resampled at coarser resolutions (2–10 m) using the aggregate function, replacing elevation values with the minimum value of the wider search window. Elevation differences between datasets were again measured using point-DEM intersections. Geospatial analyses were conducted in ArcGIS ver. 10.5.

Supplementary Materials: File 1. Data Inventory. File 2. Coastal wetland elevation survey: Shapefile of elevation points; File 3. DEM metadata.

Author Contributions: Conceptualization, writing, formal analysis, and funding acquisition, E.B.W.; data curation, L.H. and K.R.; methodology, L.H., K.R., and E.R.

Funding: This work was supported by the New Jersey Sea Grant Consortium (NJSGC) with funds from the National Oceanic and Atmospheric Administration (NOAA) Office of Sea Grant, U.S. Department of Commerce, under NOAA grant number #NA14OAR4170085, and the U.S. EPA Region 2 Wetlands Program Development Grant CD97207600. The statements, findings, conclusions, and recommendations are those of the authors and do not necessarily reflect the views of the NJSGC or the U.S. Department of Commerce [NJ-19-942].

Acknowledgments: We thank the State of New Jersey and the U.S. Fish and Wildlife Service for access to field sites, and Metthea Yepson, New Jersey Department of Environmental Protection, for assistance in the field.

Conflicts of Interest: The authors declare no conflict of interest. The funders had no role in the design of the study; in the collection, analyses, or interpretation of data; in the writing of the manuscript; or in the decision to publish the results.

References

1. Engelhart, S.E.; Horton, B.P.; Douglas, B.C.; Peltier, W.R.; Tornqvist, T.E. Spatial variability of late Holocene and 20th century sea-level rise along the Atlantic coast of the United States. *Geology* **2009**, *37*, 1115–1118. [[CrossRef](#)]
2. Church, J.A.; White, N.J. Sea-level rise from the late 19th to the early 21st century. *Surv. Geophys.* **2011**, *32*, 585–602. [[CrossRef](#)]
3. Church, J.A.; White, N.J. A 20th century acceleration in global sea-level rise. *Geophys. Res. Lett.* **2006**, *33*. [[CrossRef](#)]
4. Cazenave, A.; Palanisamy, H.; Ablain, M. Contemporary sea level changes from satellite altimetry: What have we learned? What are the new challenges? *Adv. Space Res.* **2018**, *62*, 1639–1653. [[CrossRef](#)]
5. Rahmstorf, S. A semi-empirical approach to projecting future sea-level rise. *Science* **2007**, *315*, 368–370. [[CrossRef](#)] [[PubMed](#)]
6. Kemp, A.C.; Horton, B.; Donnelly, J.P.; Mann, M.E.; Vermeer, M.; Rahmstorf, S. Climate related sea-level variations over the past two millennia. *Proc. Natl. Acad. Sci. USA* **2011**, *108*, 11017–11022. [[CrossRef](#)]
7. Hardy, R.D.; Hauer, M.E. Social vulnerability projections improve sea-level rise risk assessments. *Appl. Geogr.* **2018**, *91*, 10–20. [[CrossRef](#)]
8. Narayan, S.; Beck, M.W.; Wilson, P.; Thomas, C.J.; Guerrero, A.; Shepard, C.C.; Reguero, B.G.; Franco, G.; Ingram, J.C.; Trespalacios, D. The value of coastal wetlands for flood damage reduction in the northeastern USA. *Sci. Rep.-UK* **2017**, *7*, 9463. [[CrossRef](#)]
9. Blum, L.K.; Davey, E. Below the salt marsh surface: Visualization of plant roots by computer-aided tomography. *Oceanography* **2013**, *26*, 85–87. [[CrossRef](#)]
10. Schmid, K.A.; Hadley, B.C.; Wijekoon, N. Vertical accuracy and use of topographic LIDAR data in coastal marshes. *J. Coast. Res.* **2011**, *27*, 116–132. [[CrossRef](#)]
11. Hladik, C.; Alber, M. Accuracy assessment and correction of a LIDAR-derived salt marsh digital elevation model. *Remote Sens. Environ.* **2012**, *121*, 224–235. [[CrossRef](#)]
12. Henning, W. *User Guidelines for Single Base Real Time GNSS Positioning*; National Geodetic Survey: Silver Spring, MD, USA, 2011; 138p. Available online: https://www.ngs.noaa.gov/PUBS_LIB/NGSRealTimeUserGuidelines.v2.1.pdf (accessed on 25 March 2019).

13. Elsey-Quirk, T.; Watson, E.B.; Raper, K. Site-Specific Intensive Monitoring of Dividing Creek and Maurice River 2011–2014. Report Submitted to the Barnegat Bay Partnership and the Partnership for the Delaware Estuary. 2015. Available online: http://www.macwa.org/assets/img/com/DV_MR_2015.pdf (accessed on 25 March 2019).
14. NOAA Coastal Services Center. LiDAR Data Collected in Marshes: Its Error and Application for Sea Level Rise Modeling. 2010. Available online: <https://coast.noaa.gov/data/digitalcoast/pdf/lidar-marshes-slammm.pdf> (accessed on 25 March 2019).



© 2019 by the authors. Licensee MDPI, Basel, Switzerland. This article is an open access article distributed under the terms and conditions of the Creative Commons Attribution (CC BY) license (<http://creativecommons.org/licenses/by/4.0/>).

Modeling Regulatory Threshold Levels for Pesticides in Surface Waters from Effect Databases

Lara L. Petschick ¹, Sascha Bub ¹, Jakob Wolfram ¹, Sebastian Stehle ^{1,2} and Ralf Schulz ^{1,*}

¹ iES Landau, Institute for Environmental Sciences, University of Koblenz-Landau, D-76829 Landau, Germany; petschick@uni-landau.de (L.L.P.); bub@uni-landau.de (S.B.); wolfram@uni-landau.de (J.W.); stehle@uni-landau.de (S.S.)

² Eusserthal Ecosystem Research Station, University of Koblenz-Landau, D-76857 Eusserthal, Germany

* Correspondence: schulz@uni-landau.de

Received: 7 November 2019; Accepted: 12 December 2019; Published: 14 December 2019



Abstract: Regulatory threshold levels (RTL) represent robust benchmarks for assessing risks of pesticides, e.g., in surface waters. However, comprehensive scientific risk evaluations comparing RTL to measured environmental concentrations (MEC) of pesticides in surface waters were yet restricted to a low number of pesticides, as RTL are only available after extensive review of regulatory documents. Thus, the aim of the present study was to model RTL equivalents (RTLe) for aquatic organisms from publicly accessible ecotoxicological effect databases. We developed a model that applies validity criteria in accordance with official US EPA review guidelines and validated the model against a set of manually retrieved RTL (n = 49). Model application yielded 1283 RTLe (n = 676 for pesticides, plus 607 additional RTLe for other use types). In a case study, the usability of RTLe was demonstrated for a set of 27 insecticides by comparing RTLe and RTL exceedance rates for 3001 MEC from US surface waters. The provided dataset enables thorough risk assessments of surface water exposure data for a comprehensive number of substances. Especially regions without established pesticide regulations may benefit from this dataset by using it as a baseline information for pesticide risk assessment and for the identification of priority substances or potential high-risk regions.

Dataset: The dataset can be found in Supplemental Material <http://www.mdpi.com/2306-5729/4/4/150/s1>.

Dataset License: CC-BY-SA

Keywords: ecotoxicology; pesticide thresholds; benchmarks; environmental risk assessment; effect database; systematic filter application; exceedance rates

1. Summary

In modern agriculture, pesticides are frequently applied to minimize crop losses due to pest organisms, fungal diseases, or the growth of weeds (see Oerke [1], for review). To achieve these agronomic benefits (see Popp et al. [2], for review), pesticides as biologically active substances are regularly and globally released into the environment to treat large areas of croplands [3]. Thereby, pesticides are transported to non-target freshwater systems [4–6]. Hence, it is important to regulate pesticides and to assess the likelihood of unacceptable ecological effects in aquatic ecosystems. For instance, elaborated environmental risk assessments (ERA) are conducted for pesticides in the US, prior to granting permission of use and, at regular intervals thereafter, for reregistration (FIFRA 40 CFR [7], Part 152; [8]). For risk characterization, estimated environmental concentrations are compared to toxicity endpoints from peer-reviewed and non-peer-reviewed laboratory effect studies. Thereby, a

pesticide is characterized using different ecologically relevant surrogate species (FIFRA 40 CFR [7], Part 158; [9]). In the US, effect studies are only considered relevant for risk characterizations if they comply to certain validity criteria, as stated in the OCSPP standard test guidelines (e.g., 850.1075, 850.1010, 850.4400, 850.4500 [10–13]) and the US EPA's guidance for the review of open literature studies (e.g., treatments need to be compared to an acceptable control) [14]. The most sensitive, reliable toxicity endpoint is used to calculate risk quotients (RQ), by dividing estimated environmental concentrations by the effect concentrations. The RQ is then compared to a level of concern (LOC, in the acute risk assessment for aquatic animals: 0.5; for plants: 1) [9]. Permission for the use of an active ingredient may only be granted if the RQ does not exceed the respective LOC.

Despite elaborated risk assessment procedures, pesticides were shown to occur frequently in non-target aquatic ecosystems [15,16], where they may have detrimental effects on ecosystem structure [17], functioning [18,19], and biodiversity [20]. Therefore, post-registration monitoring of measured environmental concentrations (MEC) of pesticides in surface waters is importantly needed [16,21,22]. One traditional approach is based on toxicity endpoints of three standard species (algae *Pseudokirchneriella subcapitata*, invertebrate *Daphnia magna*, fish *Pimephales promelas*) that represent different trophic levels (e.g., Malaj et al. [23]). However, these benchmarks consider few test species only and might thus miss the most sensitive, available, and reliable endpoint on which risk evaluations should be based. Especially for some modern insecticides (e.g., neonicotinoids), it was shown that the standard test organism *D. magna* is not an appropriate proxy for the risk of invertebrates as crustaceans are 2–3 orders of magnitude less sensitive than aquatic insects (see Morrissey et al. [24], for review). Even though most likely no toxicity data is available for the most sensitive species occurring in freshwater ecosystems [25], considering all available, reliable toxicity data, such as in US ERA, is a good approach to assess risk.

Regulatory threshold levels (RTL, as introduced in [16]) are, in the present study, directly derived from the effect data (>37 species in total for 143 RTL, see Table S1) provided in regulatory documents. Their use to evaluate the risks of MEC in freshwater systems is also of ecological relevance, as RTL exceedances in the field lead to unacceptable ecological effects [16]. RTL, thus, are a valuable measure to deduce whether aquatic ecosystems are at risk due to pesticide exposure. The compilation of RTL from individual regulatory documents, however, is very time-consuming. For this reason, recent studies using RTL to evaluate MEC have been restricted to a small sample of manually collated RTL (Wolfram et al. [15], $n = 32$; Stehle and Schulz [16], $n = 28$). Albeit RTL are found in the regulatory registration documents, they cannot be easily accessed. To identify the RTL for given substances, it is necessary to (i) search online for the most recent regulatory document, (ii) check whether risk assessments were performed and sufficiently reported there, (iii) identify the relevant, reliable endpoint that was used for risk characterization, and (iv) calculate the RTL by applying the respective LOC as a safety factor. Especially steps (i) and (ii) are very time-consuming, as multiple sources where regulatory documents are listed have to be checked [26–29]. Moreover, this extensive manual search inherently lacks the ability to respond to regulatory changes, for instance, in case of a data call-in [FIFRA 40 CFR [7], Part 155] or a pesticide reregistration [FIFRA 40 CFR [7], Part 152]. Thus, it is not possible to adapt RTL collections to changes in the data basis, except via manual labor, which quickly becomes unfeasible due to the plethora of regulated pesticides (i.e., 725 US EPA registration review cases for about 1140 active ingredients published by July 2017 [30]). Given the usefulness of RTL to evaluate environmental risks [15,16], comprehensive RTL collections are urgently needed for large-scale evaluations of MEC. In principal, aquatic life benchmarks (ALB) for pesticides, provided by the US EPA on its web page [28], could be seen as such a collection. However, although ALB are available for a considerable number of pesticides ($n = 486$), they show two major drawbacks. First, the list of ALB is updated irregularly, second, ALB do partly not relate to the newest regulatory documents. Data errors (i.e., incorrect RTL) have thus been found in about 25% of an evaluated subsample of ALB ($n = 143$, own evaluation, see Appendix B for details). Therefore, the aim of the present study was to develop and validate a model that derives estimated RTL equivalents (RTL_e) for freshwater organisms

for a broad number of pesticides and that can be used for scientific risk evaluations. This model is based on two publicly accessible databases maintained by the US EPA: The US EPA ECOTOXicology knowledgebase (ECOTOX, <https://cfpub.epa.gov/ecotox/index.cfm>) [31] and the Office of Pesticide Programs Pesticide Ecotoxicity Database (OPP, <https://ecotox.ipmcenters.org>) [32]. Both databases contain a large number of effect studies (ECOTOX: ~940,000 entries; OPP: ~32,000 entries) and are relevant for the US ERA (also see Section 3.1). However, the quality of the studies listed in the databases varies substantially, so that not all studies reliably describe the toxicity of pesticides. To exclude studies that are unlikely to be used in ERA due to low reliability, filter criteria were formulated based on the provided information on test characteristics (see Tables A1 and A2) and in accordance with official validity criteria [10–14,33]. One rather theoretical approach to systematically filter large aquatic toxicity databases was, for instance, published by Beasley et al. (i.e., SIFT method) [34], and was recently applied to a large set of collected aquatic toxicity data with a focus on industrial chemical risk assessment [35]. In the present study, we developed a similar approach focusing on pesticide risk assessment by translating official validity criteria from standardized test protocols [10–13,33] and the US EPA guideline for the review of open literature studies [14] into an SQL code. Criteria considered from the test protocols included, e.g., study durations, measured effect type, and endpoint type for the respective organism group. From the EPA guideline, e.g., proper control, chemical analysis, and physical units have been extracted. The SQL code was used to query local versions of the ECOTOX and OPP databases. After filter application, the remaining studies were used for threshold estimations (i.e., RTLe) based on the most sensitive, available endpoint, as done during manual RTL derivation [16]. To set up the model, different combinations of filter criteria were tested and evaluated in terms of the precision of estimates (basic, mid, and full model, Tables A1 and A2, Figures A1–A3). To evaluate the precision of the modeled RTLe, the estimated threshold levels were compared to 94 manually retrieved RTL (i.e., the calibration dataset). The model was validated by comparing the RTLe/RTL ratios of the calibration data ($n = 94$, see Table S1) to the RTLe/RTL ratios of an independent set of pesticides (i.e., validation dataset, $n = 49$, see Table S1). Furthermore, we demonstrate in a case study using 27 insecticide compounds, how RTLe can be used in actual risk evaluations. The RTLe model resulted in 1283 RTLe, 676 RTLe of pesticides (i.e., fungicides, herbicides, insecticides) plus 607 of other chemicals (see 2.1, Table S2) that might also be of interest for environmental evaluations. This list will be regularly updated to reflect potential changes in the underlying effect databases.

With the present study, we have developed, validated, and applied a dynamic model that estimates a large number of RTLe for freshwater systems based on reproducible validity criteria. With the compiled list of RTLe, comprehensive evaluations of pesticide monitoring data and associated risks in surface waters are enabled for the first time for a large number of pesticides, as well as further chemicals with potential environmental impacts.

2. Data Description

2.1. The Dataset

The dataset contains RTLe for freshwater organisms for 1283 chemicals in ug/L (Table S2). A classification into use types applying the MAGIC graph [36] revealed that 676 of these substances are used as pesticides (herbicides, fungicides, or insecticides). Further, 260 substances were classified as other chemicals (e.g., microbiocides, solvents, plant growth regulators, repellents) and 347 substances remained unclassified. In addition, the CAS number, RTLe, source database, and use type classification are provided (Table 1). In addition to the publication of a Microsoft Excel® spreadsheet containing the compiled data, by which the most recent version of the dataset becomes accessible for the public (<https://static.magic.eco/rtle2>), all RTLe will be added to the MAGIC graph [36] and are available through the chemical search interface (<https://static.magic.eco/rtle1>), and updated there regularly.

Table 1. Overview over the published dataset.

Column	Explanation
CAS Number	Chemical abstract service identifier
RTLe	Estimated regulatory threshold level [ug/L]
Database	Source of the presented RTLe, i.e., ECOTOX database, OPP database
Classification	Fung = fungicides, Herb = herbicides, Ins = insecticides, Other = other category according to MAGIC graph [36] classification, Unclassified = no classification

2.2. Data Quality

The RTLe from the calibration dataset ($n = 94$, Table S1) were validated against an independent sample of RTL ($n = 49$, Table S1) to test the model's performance. Model transferability was confirmed by non-parametric hypothesis testing (Wilcoxon rank sum test: ECOTOX database: $W = 2148.5$, $p = 0.628$; OPP database: $W = 1527.5$, $p = 0.474$), which showed no significant difference in predictive accuracy between calibration and validation data (Figure 1, Figure A5). The proportion of RTLe that correctly estimated the RTL after combining the queries of both databases (Figure 1) was 48.9%. Further, 95.6% of RTLe were within ± 1 orders of magnitude, while 87.6% lay within ± 0.5 orders of magnitude (i.e., a factor of 3.2). Thus, for the vast majority of data, minimal deviance from official RTL can be assumed, underlining the robustness of the presented model. Estimates for only few substances ($n = 5$, i.e., tebufenozide, fenthion, heptachlor, methyl-parathion, sulfometuron-methyl) underestimated the RTL by more than 0.5 orders of magnitude. Whenever the RTL was underestimated, this means that a more sensitive endpoint was listed in the databases for which the applied exclusion criteria did not apply. This might be due to expert judgements, as these remaining endpoints after filter application were probably omitted during regulatory risk characterizations by risk assessors for reasons currently not reflected by the model (as not all relevant test characteristics are consistently encoded in the databases). As this was the case for only a few substances (Figure 1, $RTLe/RTL < 1$), the overall probability to underestimate the RTL remains low.

Albeit model estimates were on average significantly higher (based on 95% CIs) than the original RTL (bootstrapped mean with 95% CI: 1.21 (1.04–1.42 95% CI; median = 1)), RTLe would rather underestimate the risk if used in risk evaluations, resulting in a low likelihood of false-positive risk indications. Since only 88 (ECOTOX database) and 78 (OPP database) of the relevant, most sensitive endpoints for the 143 manually retrieved RTL were included in the respective databases (i.e., exact match between the endpoints used for RTL and RTLe compilations), correct estimates were inherently not achievable for all pesticides. However, for some pesticides, deviations were only marginal (deviation $< \pm 0.1$ orders of magnitude, excluding 0, $n = 16$ (ECOTOX database) and $n = 26$ (OPP database)). In some cases, the underlying endpoints might still originate from the same study (identifiable by the reported study ID and same test organism), e.g., in case of tribufos, methiocarb, and formetanate HCl. For instance, the minor deviations could result from the rounding of endpoints if different numbers of digits behind the comma were reported in the document and the database (as likely for formetanate HCl; 0.09 parts per million (ppm) in the document [37], and 0.0868 parts per million in the OPP database). Larger deviations could, however, be based on recalculations of endpoints by EPA staff (e.g., to account for the percentage of active ingredient if original studies were conducted with formulations). Additionally, it became apparent that endpoints were more likely to not be included in the respective database the newer the regulatory document was (see Figures A6 and A7). Hence, there appears to be a time-lag between the update of the databases and the publication of regulatory documents.

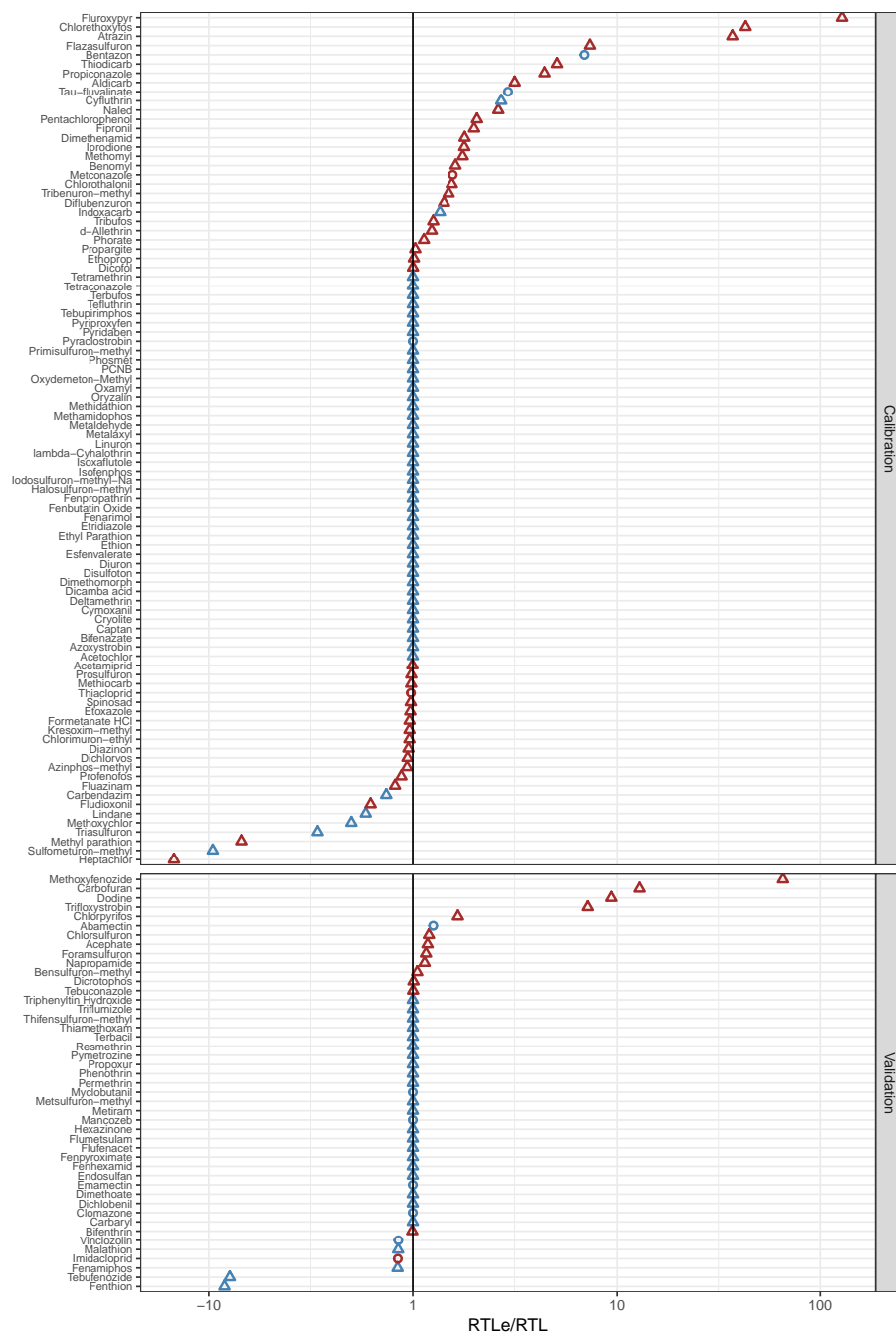


Figure 1. Precision of the final regulatory threshold level equivalent (RTL_e) model expressed as RTL_e to RTL ratio (log₁₀-transformed) for the calibration and validation datasets (n = 137). The one line indicates where RTL are estimated correctly (RTL = RTL_e). A ratio < 1, shows an underestimation of the RTL by the RTL_e, a ratio > 1 an overestimation. Triangles indicate whether RTL_e were based on data provided in the Office of Pesticide Programs Pesticide Ecotoxicity Database (OPP); circles refer to the US EPA ECOTOXicology knowledgebase (ECOTOX). Not all relevant endpoints that were listed in the regulatory documents were also listed in the respective databases. Pesticides, with included endpoints are displayed in blue, pesticides without the listed, most sensitive, relevant endpoint in the respective database are displayed in red.

If only pesticides with a relevant, most sensitive endpoint that is also included in the database were considered, the precision of estimates improved significantly. A strong association between the two variables was indicated as the bootstrapped mean ratio approached 1 (mean ratio RTL_e/RTL

of 0.94 (0.84–1.05 95% CI; median = 1)) and minimal deviations for the majority of pesticides were observed (Figure 1). Additionally, RTLe for pesticides whose relevant, most sensitive endpoint for RTL compilation was not included in the databases tend to overestimate the RTL (i.e., $RTLe/RTL > 1$) with a bootstrapped mean ratio with 95 CI of 1.75 (1.27–2.48 95% CI; median = 1.16). These additional analyses demonstrate a good performance of the model particularly for the pesticides with the included relevant endpoint for RTL compilation, indicated by a high precision of estimates. For relevant, most sensitive endpoints from the regulatory document, that were used for RTL compilation but were not included in the respective databases, even though it was inherently not possible to obtain correct estimates, RTLe rather overestimated the RTL. Hence, the use of these RTLe would not result in false positive risk estimations. Thus, overall, the model precision is high with a tendency to slightly overestimate the RTL. Consequently, based on the uncertainty associated with these modeled thresholds, ecological effects in surface waters could also occur at concentrations below the respective RTLe, and are very likely if RTLe are exceeded (cf. Stehle and Schulz [16]).

2.3. Case Study

The model was applied for 27 insecticides from an extensive dataset of quantified (i.e., \geq limit of quantification) insecticide surface water concentrations (i.e., MEC, $n = 3001$, 1962–2017) in the United States described in detail in Wolfram et al. [15]. The RTLe for the insecticides used in this case study are, in terms of model precision, a representative sample of all RTLe, for which the model was calibrated and validated (Wilcoxon rank sum test: $W = 1429$, $p = 0.749$). Risk evaluation (i.e., the calculation of exceedance rates) of MEC using RTLe showed only marginal differences of 3.8% (95% CI 2.2–5.4) if compared to the evaluation of MEC using RTL. In detail, bootstrapped median exceedance rates lay at 55.8% (95% CI 51.8–59.8) and 52.0% (95% CI 48.0–56.0) if insecticide MEC were compared to RTL and RTLe, respectively (Figure 2). No statistically significant difference (based on 95% CIs) between the exceedance rates were observed if MEC were compared to RTL or RTLe. This underlines the model's ability to accurately identify environmental risks. However, using RTLe, the risk was slightly underestimated, such that using the modeled thresholds resulted in a less conservative risk evaluation (blue line, Figure 2). In conclusion, we found it being representative of the entirety of RTLe and providing comparable risk evaluation based on actual field measurements.

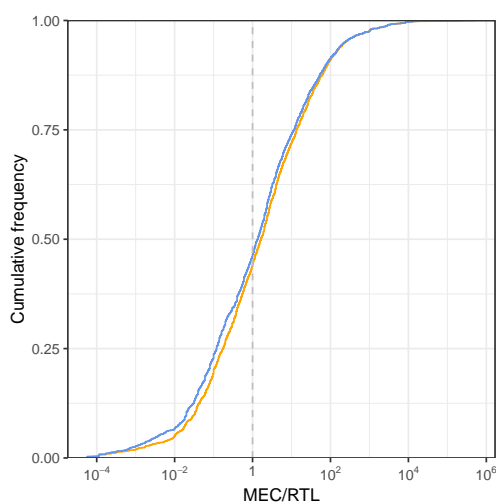


Figure 2. Cumulative risk distribution for measured environmental concentrations (MEC, $n = 3001$) of 27 insecticides in US surface waters (see Wolfram et al., 2018) compared to RTL (orange line) and RTLe (blue line), respectively. The vertical dashed line indicates where MEC equals RTL or RTLe. Above a ratio MEC to RTL or RTLe of 1, MEC exceeded the threshold. The proportion of exceeded MEC ($\log_{10}(MEC/RTL) > 1$) lies at 0.56 (bootstrapped 95% CI 0.52–0.60) and 0.52 (bootstrapped 95% CI 0.48–0.56) for RTL and RTLe, respectively.

3. Methods

3.1. The Databases

The present study was based on two publicly accessible effect databases maintained by the US EPA (i.e., ECOTOX database and OPP database, see Figure A1), as introduced in Section 1. The ECOTOX database contains predominantly peer-reviewed, open literature studies of ecotoxicological effects on a variety of test organisms for individual substances. The OPP database contains data from peer-reviewed and non-peer-reviewed studies that were previously reviewed by the US EPA for risk characterizations within the process of pesticide regulations, also for a variety of test organisms. The OPP database is more aggregated than the ECOTOX database (i.e., contains less information for individual studies). Therefore, the possibility to formulate filter criteria (Tables A1 and A2) to select only valid endpoints was limited to the provided information. However, since EPA staff already rated the reliability of these studies as invalid, supplemental and core, relevant endpoints can be selected by excluding invalid studies, as only supplemental and core studies are used for ERA by the US EPA [9]. Both databases were downloaded and imported into a relational database management system (PostgreSQL, pgAdmin 4.1; latest database updates: ECOTOX: 06/2019; OPP: 03/2017). Data was analyzed using R [38], and the following packages [39,40].

The test medium was used as a criterion to distinguish freshwater organisms from saltwater/estuarine organisms to enable the estimation of RTL for freshwater systems. As the OPP database does not provide information on the test medium, unlike the ECOTOX database (e.g., freshwater, saltwater), the typical, predominantly used test media were retrieved from the ECOTOX database by joining species and media tables by species name. All test media for species that were not listed in the ECOTOX database but occurred in the OPP database ($n = 61$), were inferred from the predominant habitat specified, as specified in additional sources (e.g., WoRMs database (<http://www.marinespecies.org>), Algaebase database (<https://www.algaebase.org>), Stephen et al. [41–43]).

3.2. Collection of RTL

A list of 143 RTL (updated by October 2018) used for model validation and calibration was compiled by reviewing the respective, most recent regulatory documents provided by the US EPA from different sources [26–29]. Active substances were either searched by CAS number or name to unambiguously identify each test substance. Pesticides for the present studies were chosen based on previous work [15,16], use data [44] and the availability of regulatory documents on the searched sources covering different important use types (i.e., fungicides, herbicides, and insecticides). Once the most recent documents were identified and downloaded, RTL were computed similar to the methods described in Stehle and Schulz [16] as follows: First, the valid ecological effect data for freshwater organisms, that was used for risk quotient (RQ) calculations within the respective document, was identified. As the model was supposed to be calibrated for active ingredients, only studies performed with the active ingredient of a pesticide were selected. Further, only definite endpoints (without the qualifiers “>” and “<”) were considered to be relevant. If no information on RQ calculations were provided but sufficient ecological effect data was listed, the relevant endpoint was chosen based on the US EPA’s classification of endpoints as supplemental and core (excluding invalid studies). This follows the procedure of endpoint selection by the US EPA during the screening of available data for ERA [9]. As a final verification of the manually selected endpoint, written justifications of endpoint selections, if available, were checked to confirm the identified species and effect endpoint. Finally, as the most sensitive species drives regulatory decisions [9], the lowest, valid endpoint was selected for RTL computation. These RTL were calculated by multiplying the selected, most sensitive, relevant endpoint by the respective level of concern (LOC; 0.5 for acute aquatic animal studies, 1 for aquatic plant studies) [9]. The final dataset of RTL was divided randomly into a calibration dataset ($n = 94$) and a validation dataset ($n = 49$) to set up the model.

3.3. Model Building and Calibration

To set up the model, a basic, mid, and full model were tested differing in the strictness of applied filter criteria for each database separately. The basic model was set up containing elementary filter criteria to define a basic dataset (basic model, see Tables A1 and A2, and Figure 3). Then, based on the most sensitive, remaining endpoint per substance, RTLe were calculated for the substances of the calibration dataset (see Section 1. Summary). The application of the basic models would result in a large underestimation of the RTL (i.e., overestimating risks), as for 90% and 66% of the substances for the ECOTOX and OPP database, respectively, the RTLe would be estimated too low if compared to the RTL. At the same time, the proportions of correct estimates (2% and 21%) and overestimates (8% and 13%) were rather low, such that this query would not result in accurate RTL estimates. To improve model precision, additional filter criteria (Tables A1 and A2) were formulated based on quality standards [10–14,33], as introduced in Section 1, to identify and exclude data with a low reliability (i.e., which are likely to be rejected during regulatory risk assessments). A mid model containing essential criteria (mid model, $n = 4$, for the ECOTOX and OPP database, respectively; see Tables A1 and A2) was set up and RTLe were calculated and compared to RTL to evaluate the precision of estimates. Applying the mid model, model precision improved, as 28% and 42% of the RTLe were estimated correctly, 54% and 34% of RTLe underestimated their RTL and 17% and 24% of RTLe exceeded their RTL, for the ECOTOX and OPP database, respectively. For further refinements, additional criteria were formulated to build a full model, which contains a total of 17 and 8 consecutive filter criteria for the ECOTOX and the OPP database, respectively (full model, Tables A1 and A2). Here, the model performance could again be improved, as 43% and 47% of the RTLe were estimated correctly, only 25% and 24% of RTLe underestimated their RTL, and 32% and 29% of RTLe exceeded their RTL, for the ECOTOX and OPP database, respectively (see Section 2.2 Data quality and Section 2.3 Case study for further details on the precision of estimates). Thus, calibration aimed at increasing the proportion of correct estimates ($RTLe/RTL = 1$) while decreasing the proportion of substances for which the RTLe would underestimate the true RTL ($RTLe/RTL < 1$, see Figure 3). Consequently, the comparison of RTLe to MEC would be unlikely to result in a false positive overestimation of the risk.

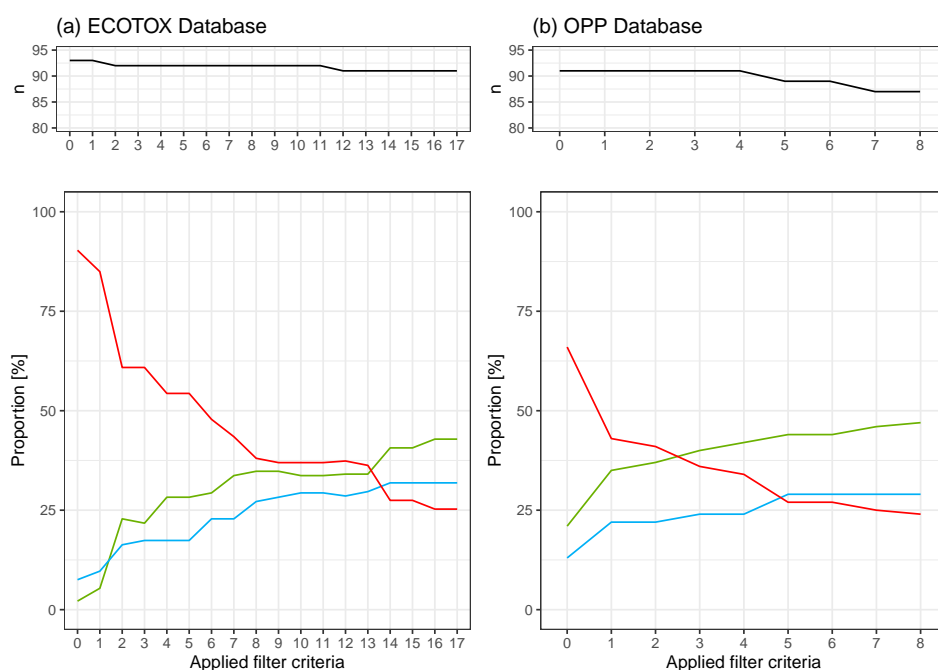


Figure 3. Overview of the influence of applied filter criteria (Tables A1 and A2) on the remaining number of pesticides for which RTLe could be estimated for the ECOTOX database (a) and the OPP database (b), respectively. Upper panels show the remaining number of pesticides, lower panels the proportions of RTLe that were estimated correctly (green lines), estimated too high (blue line), or too low (red line).

As a consequence of filter refinements, the application of each additional filter step resulted in a minimal loss of endpoints (see Figures A2–A4) of lower reliability. In this process, for some substances, all data was lost, such that no final RTLe could be estimated (calibration dataset: $n = 94$ pesticides; null model estimates: $n = 93$ and 91 pesticides; full model estimates: $n = 91$ and 87 pesticides, respectively, for the ECOTOX and OPP database). This was a trade-off, where improving the model precision was preferred over maximizing the generation of RTLe.

3.4. Model Validation and Join of ECOTOX and OPP Query Results

The model was validated on two levels: (i) The measure of precision ($\log_{10}(\text{RTLe}/\text{RTL})$) for calibration and validation data was compared by hypothesis testing to test whether the precision of estimates was statistically different when the model was applied to an independent set of pesticides. In case of non-normality and heteroscedasticity, non-parametric testing was conducted (i.e., Wilcoxon Rank Sum test, see Section 2.2 for results). Then, (ii) it was tested whether external factors (i.e., number of available endpoints prior to filter application, publication year of the most recent regulatory document, use type of the pesticide) had an influence on the model precision by either hypothesis testing or testing for correlations. The number of available endpoints per substance had no influence on the precision of estimates (Spearman's rank correlation rho: ECOTOX database: $S = 450,422$, $p = 0.389$, $\rho = -0.074$; OPP database: $S = 308,287$, $p = 0.558$, $\rho = 0.052$). Further, the test of a potential association between the publication year of the regulatory document and the measure of model precision revealed that RTL from newer studies were more likely to be overestimated (significant for ECOTOX database estimates: $S = 316,508$, $p = 0.004$, $\rho = 0.245$; not significant for OPP database estimates: $S = 300,311$, $p = 0.391$, $\rho = 0.077$). Further, the RTL based on endpoints reported in newer publications were less likely to be included in the respective database (see Figures A6 and A7). Thus, there appears to be a delay in the update of the databases. Finally, the test for differences between the estimates for different use types (i.e., herbicides, fungicides, and insecticides) revealed no significant differences (Kruskal–Wallis rank sum test: Kruskal–Wallis chi-squared: 3.64 , $df = 2$, $p = 0.16$). This was confirmed by a post-hoc pairwise Wilcoxon rank sum test. Thus, it was concluded, that the precision of the model does neither rely on the number of endpoints available for the respective pesticide, nor on the use type. However, dependencies became apparent for the publication year and the presence of the most sensitive, relevant endpoint used for RTL compilation in the respective database. That means that RTL were more likely to be estimated too high for newer publications and non-included endpoints (see Figures A6 and A7).

After the model was successfully validated, the final dataset of RTLe (Table S2) was compiled by pooling the calibration and validation data and merging the estimates from the different databases: The ECOTOX data was joined to the OPP data, whereby all RTLe from the OPP database were kept. Here, OPP estimates were preferred over ECOTOX estimates, as the classification into core, supplemental, and invalid studies allowed to exclude invalid studies with a higher degree of confidence than in the ECOTOX database. Thus, the OPP dataset was complemented with ECOTOX data, for which no OPP-RTLe was available.

3.5. Bootstrapped Model Precision

Model precision was estimated by bootstrapping mean ratios (RTLe/RTL , $n = 1000$), where a mean close to 1 would indicate a high model precision. Vice versa, the larger the departure from 1, the higher the imprecision. While a mean ratio < 1 indicates that estimates would rather be too low and the model would result in too sensitive thresholds, a mean ratio > 1 would indicate conservative threshold estimates. Ratios were sampled from the final dataset (combination of OPP and ECOTOX estimates) with replacements of the same size as the original dataset and with 1000 repetitions (Monte Carlo resampling) following methodologies as outlined in [45,46]. Then, from the bootstrapped samples of ratios, the mean ratio, median ratio, and 95% confidence limits as 0.025 and 0.975 centiles (percentile method, e.g., [45]) were computed.

Further, it was tested whether the endpoints leading to the RTL for all substances were included in the respective databases such that correct estimates would be theoretically possible. By again bootstrapping mean ratios of RTLe to RTL, it was tested whether model precision improved if only pesticides were considered, whose relevant endpoint actually occurred in the respective database.

3.6. Model Application

For the final model queries, the seventeenth and eighth filter criteria for the ECOTOX and OPP databases, respectively, were removed as it was no longer necessary to restrict the results to the years of publication. These filter criteria were only used for calibration and validation of the model, as potentially occurring endpoints introduced into the databases after the publication of the regulatory documents could not yet be included to regulatory risk characterizations and would thus bias the model precision.

The final list of RTLe will be updated regularly and included to the magic graph (see <https://static.magic.eco/rtle1> and <https://static.magic.eco/rtle2>), as the ECOTOX database is updated four times a year. Simultaneously, the OPP is checked for updates, whenever the ECOTOX database is updated such that the dataset, on which the model and thereby the RTLe are based, cover the latest studies added to the effect characterizations.

Here, the risk assessment procedure was applied to all substances listed in the ECOTOX database and OPP database, as both databases are relevant to the risk assessment process of pesticides. However, beside the 676 RTLe for pesticides, additional RTLe for chemicals of other use types are returned by the model. These might be of special interest to complement scientific risk evaluations, as the model enables the direct comparison of pesticides to other use types based on uniformly derived thresholds.

3.7. Case Study

To evaluate the likelihood to over- or underestimate the risk if exceedance rates are calculated by comparing MEC to RTLe instead of RTL, we performed a case study based on $MEC \geq$ quantification limits as reported by Wolfram et al. [15] ($n = 3001$ MEC for 27 insecticides). First, risk distributions [16] obtained by using RTL and RTLe, as well as the resulting exceedance frequencies, were compared descriptively. In addition, to test for significant differences in median exceedance rates, we used bootstrap methods to calculate medians with 95% confidence limits [46,47]. Therefore, we sampled 500 MEC with replacements and 1000 repetitions from this dataset to estimate median exceedance rates. Then, for each resampled dataset, the proportion of MEC exceedances was calculated for RTL and RTLe, respectively. From the resulting bootstrapped distributions of exceedance rates, the median with confidence limits were calculated by taking the 0.025, 0.5, 0.975 centiles (i.e., percentile method, e.g., [45]). Additionally, the median difference (in percent points) between the exceedance rate of MEC compared to RTL and RTLe, respectively, was bootstrapped with confidence limits.

To ensure that RTLe used in this case study ($n = 27$) are representative for the entirety of RTLe from the pooled data (i.e., calibration and validation data, $n = 137$) in the study, we used hypothesis testing (i.e., Wilcoxon Rank sum test) to test for significant differences between the aforementioned data subset and pooled dataset.

4. User Notes

RTLe can be used to evaluate pesticide MEC and to calculate exceedance rates (for methods see [15,16]). They are intended for use in large scale analyses over a large number of substances where, despite deviations for individual substances, a reasonable statistical certainty can be achieved (see Section 2.2 Data quality). For studies with only a few substances, consultation of the respective regulatory documents should be considered.

Supplementary Materials: The following are available online at <http://www.mdpi.com/2306-5729/4/4/150/s1>. Table S1: aux_rtl.xlsx; Table S2: RTLe_V01.xlsx.

Author Contributions: Conceptualization, L.L.P.; Methodology, L.L.P., S.B., and J.W.; Software, L.L.P. and S.B.; Validation, L.L.P., J.W., and S.B.; Formal analysis, L.L.P.; Investigation, L.L.P., R.S., and S.S.; Resources, R.S.; Data curation, L.L.P. and S.B.; Writing—original draft preparation, L.L.P.; Writing—review and editing, L.L.P., S.B., J.W., S.S., and R.S.; Visualization, L.L.P. and J.W.; Supervision, R.S. and S.S.; Project administration, R.S. and S.S.; Funding acquisition, R.S.

Funding: This research was funded through a scholarship by The Deutsche Bundesstiftung Umwelt DBU (German Federal Environmental Foundation) to L.L.P. and by the German Society for the Advancement of Sciences (DFG SCHU 2271/6-2).

Conflicts of Interest: The authors declare no conflict of interest.

Appendix A

Table A1. ECOTOX database filter criteria.

Filter Criteria	Description	Model
0	Basic filter criteria, that select studies with a concentration larger than 0, convertible to ug/L, and conducted with freshwater medium. Further, a concentration must be specified, and not include "NR", "ca", ">", "~", or "x".	Basic
1	The test type needs to be specified as "acute" or "not coded".	Mid
2	Only acute endpoint types are selected, that describe a concentration at which an effect occurs for 50% of the tested organisms (i.e., LC ₅₀ , EC ₅₀ , IC ₅₀)	Mid
3	For animals, mortality and intoxication are allowed as effects; for plants, growth, reproduction, and population effects are selected.	Mid
4	The exposure duration should be one of the following: For animals: 48, 72, 96 h, 2, 3, 4 d for plants: 120 h, 5, 7, 14 d	Mid
5	Exclude studies with multiple measurements.	Full
6	Exclude studies with effect comments.	Full
7	The test substance purity should have a minimum of 70% active ingredient or specified as not coded not reported.	Full
8	Tests should be conducted with active ingredients, such that the concentration type should be the active ingredient or specified as not coded or not reported.	Full
9	Only laboratory studies are considered relevant.	Full
10	Certain formulations are excluded by name (e.g., IN-MP819, INJT333, DPX-KN125, INU8E24, INUYG24)	Full
11	The organism's source should not be specified as wild or multiple.	Full
12	Only definitive endpoints are considered relevant.	Full
13	The test method must be specified.	Full
14	A chemical analysis must be conducted.	Full
15	The test should have been conducted with a proper control.	Full
16	Test organisms characterized with '> 24 h', '>24 h', or 'Fry' and tests conducted with the larval life stage of <i>Macrobrachium rosenbergii</i> are excluded.	Full
17	The publication year of the regulatory document needs to be older or equal to the reference year for the respective study. ¹	Full

¹ Only applicable for calibration and validation of the data.

Table A2. OPP database filter criteria.

Filter Criteria	Description	Model
0	Basic filter criteria, that select studies with a concentration larger than 0, convertible to ug/L, and conducted with freshwater medium. Further, a concentration must be specified, and not include "NR", "ca", ">", "~", or "x".	Basic
1	Only acute endpoint types are selected, that describe a concentration at which an effect occurs for 50% of the tested organisms (i.e., LC ₅₀ , EC ₅₀ , IC ₅₀)	Mid
2	The exposure duration should be one of the following: For animals: 48, 72, 96 h for plants: Lower or equal to 336 h	Mid
3	Studies should be rated as supplemental or core.	Mid
4	Only definitive endpoints are considered relevant.	Mid
5	Certain formulations, or metabolites are excluded by name (e.g., IN-MP819, INJT333, DPX-KN125, weed killer, product, formulation, metabolite)	Full
6	The guideline should not be specified as NG (no guideline)	Full
7	The test substance purity should have a minimum of 70% active ingredient.	Full
8	The publication year of the regulatory document needs to be older or equal to the reference year for the respective study. ¹	Full

¹ Only applicable for calibration and validation of the data.

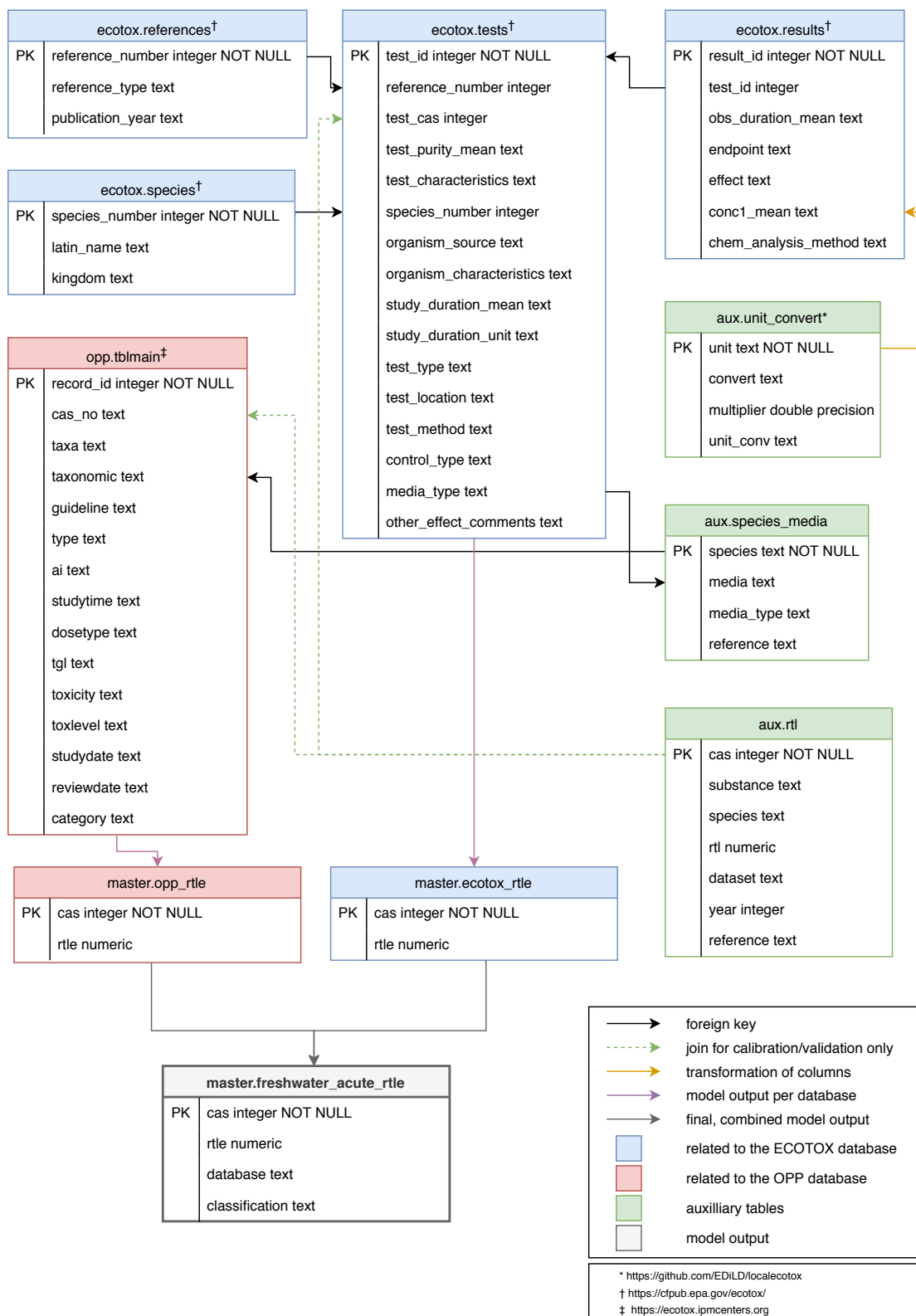


Figure A1. Overview on the relationships between the databases and tables on which the model is based. The data from the master.freshwater_acute_rtle table (S2, file name: RTLe_V01.xlsx) and the aux.rtl table (S1, file name: aux_rtl.xlsx) are published as Supplemental Material.

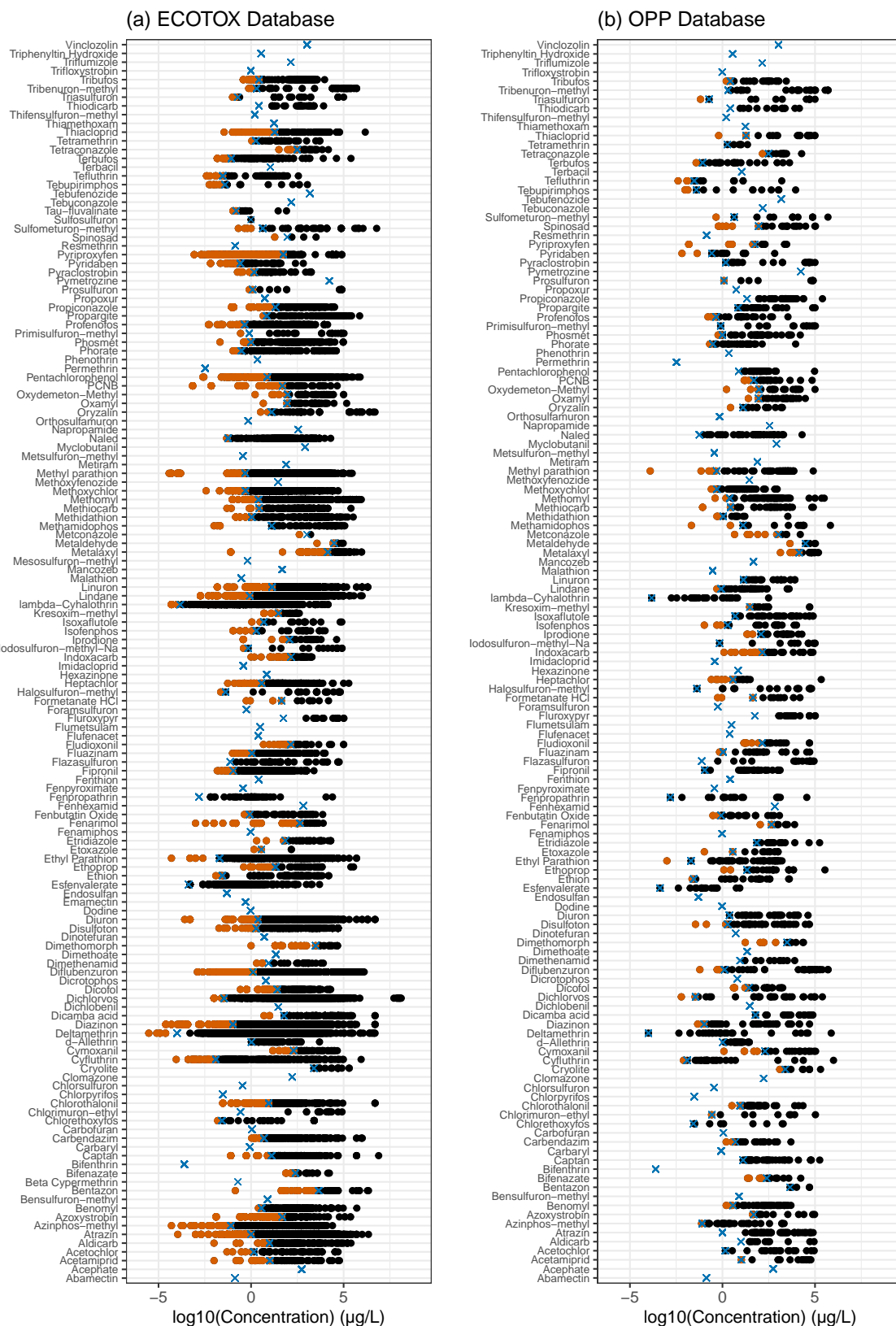


Figure A2. Distribution of remaining endpoints after basic model application for the ECOTOX database (a) and the OPP database (b). Orange dots indicate endpoints that are more sensitive than the relevant endpoint used for RTL compilation. Blue crosses indicate the relevant endpoint for RTL compilations and black dots indicate endpoints that are less sensitive than the relevant endpoint used for RTL compilations.

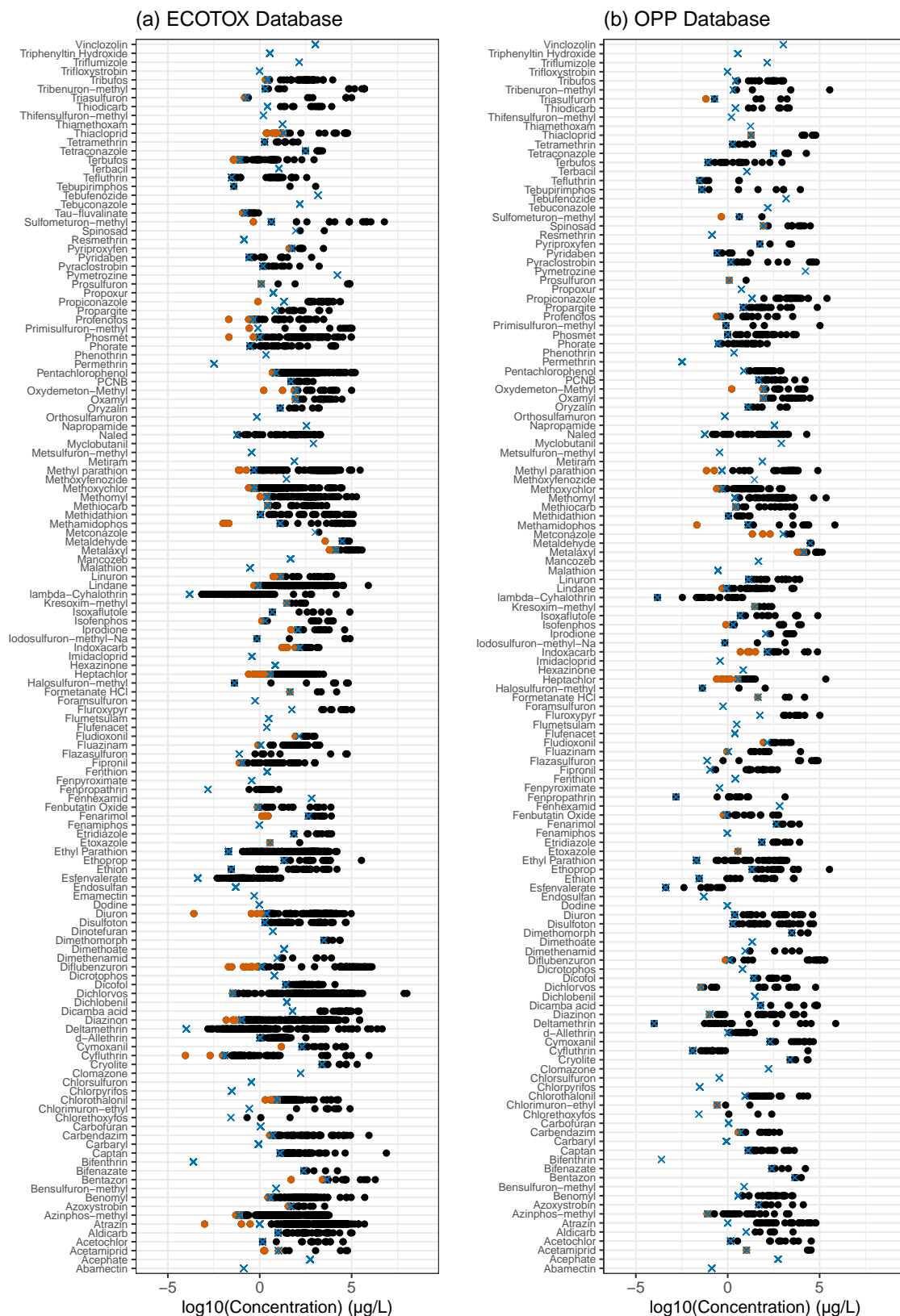


Figure A3. Distribution of remaining endpoints after mid model application for the ECOTOX database (a) and the OPP database (b). Orange dots indicate endpoints that are more sensitive than the relevant endpoint used for RTL compilation. Blue crosses indicate the relevant endpoint for RTL compilations and black dots indicate endpoints that are less sensitive than the relevant endpoint used for RTL compilations.

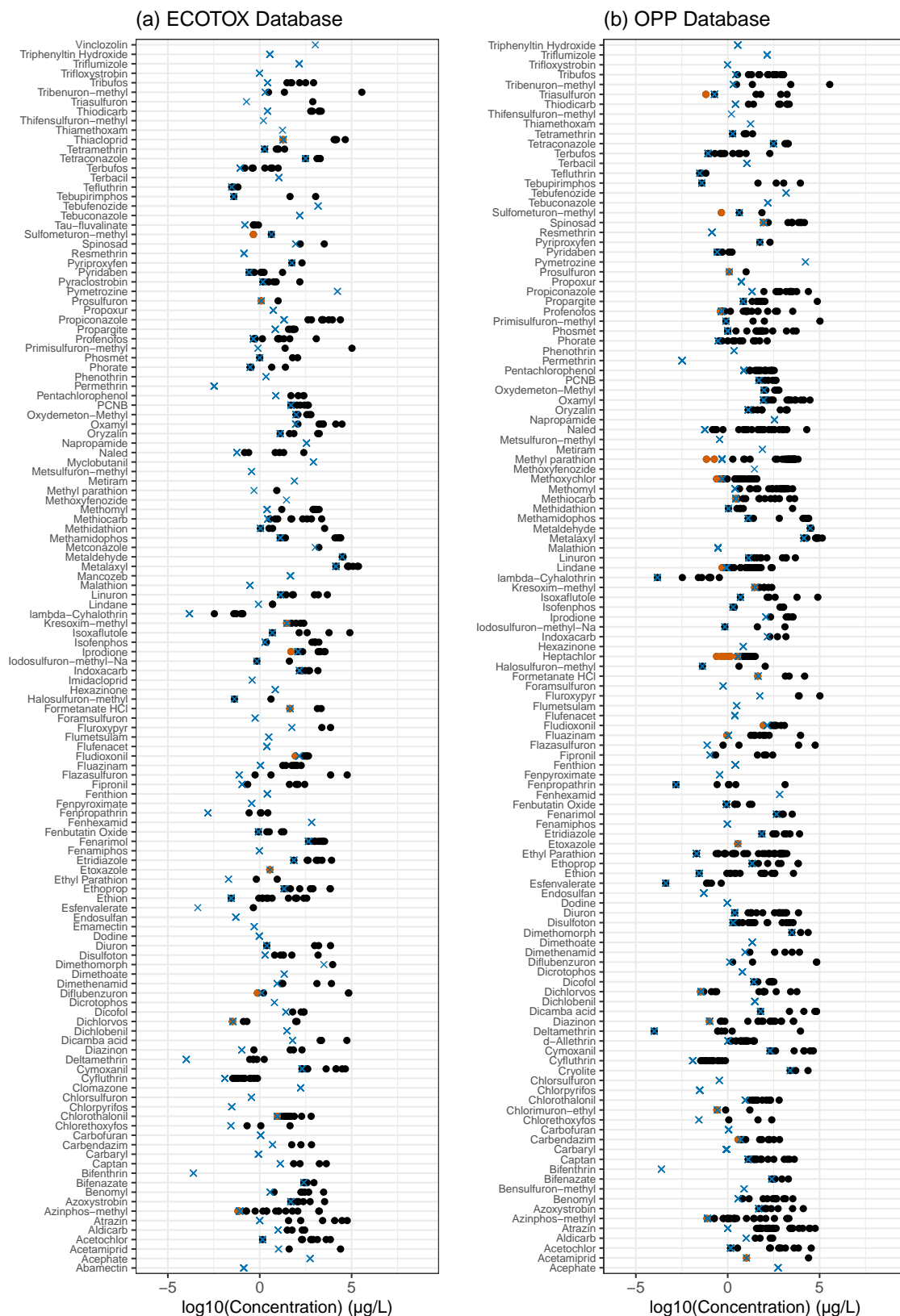


Figure A4. Distribution of remaining endpoints after full model application for the ECOTOX database (a) and the OPP database (b). Orange dots indicate endpoints that are more sensitive than the relevant endpoint used for RTL compilation. Blue crosses indicate the relevant endpoint for RTL compilations and black dots indicate endpoints that are less sensitive than the relevant endpoint used for RTL compilations.

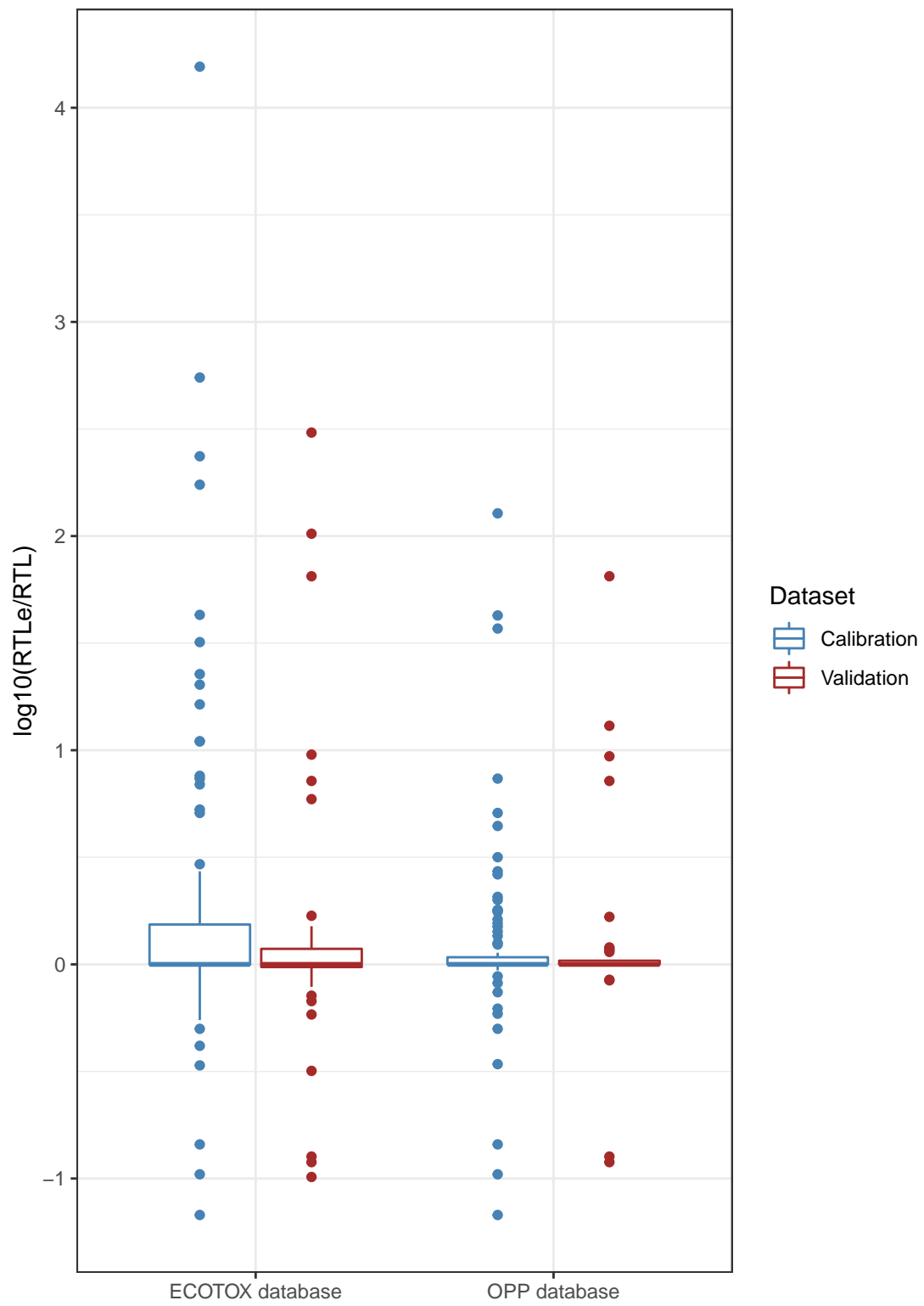


Figure A5. Comparison of model precision (expressed as log10 ratio of RTLe to RTL) for calibration and validation data based on ECOTOX and OPP database estimates.

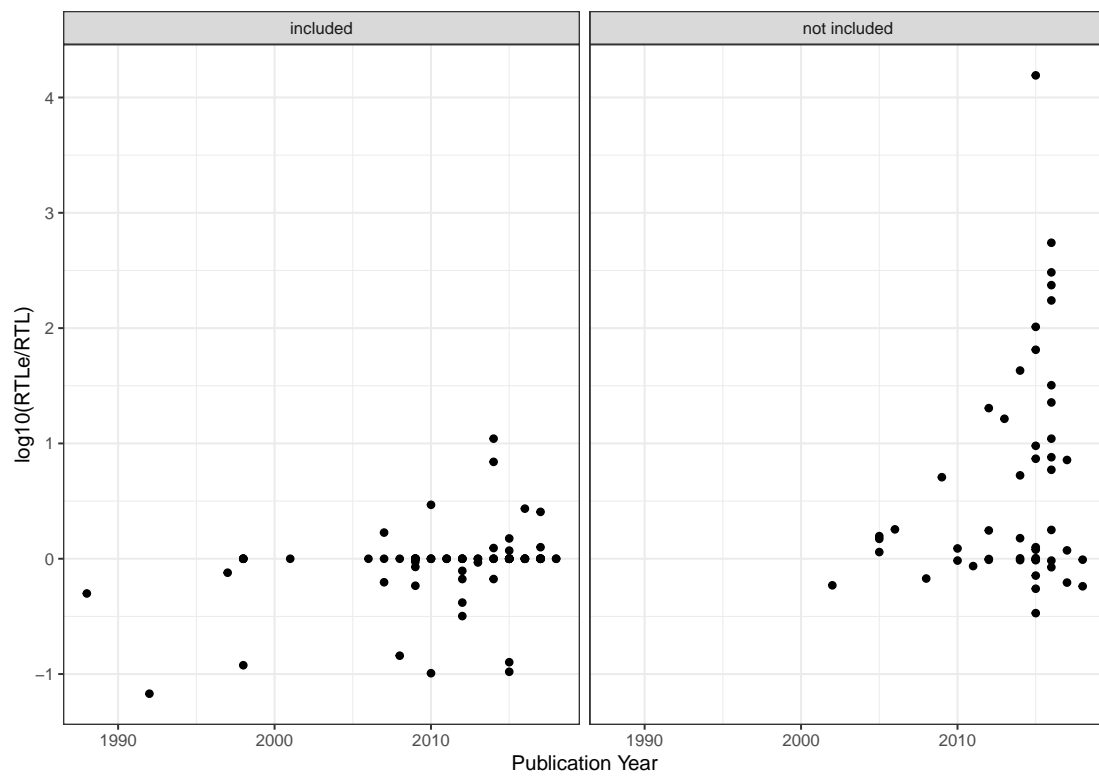


Figure A6. Comparison of model precision (expressed as \log_{10} ratio of RTLe to RTL) for ECOTOX database estimates in dependence on the publication year of the regulatory document for RTL that were included in the database and not included.

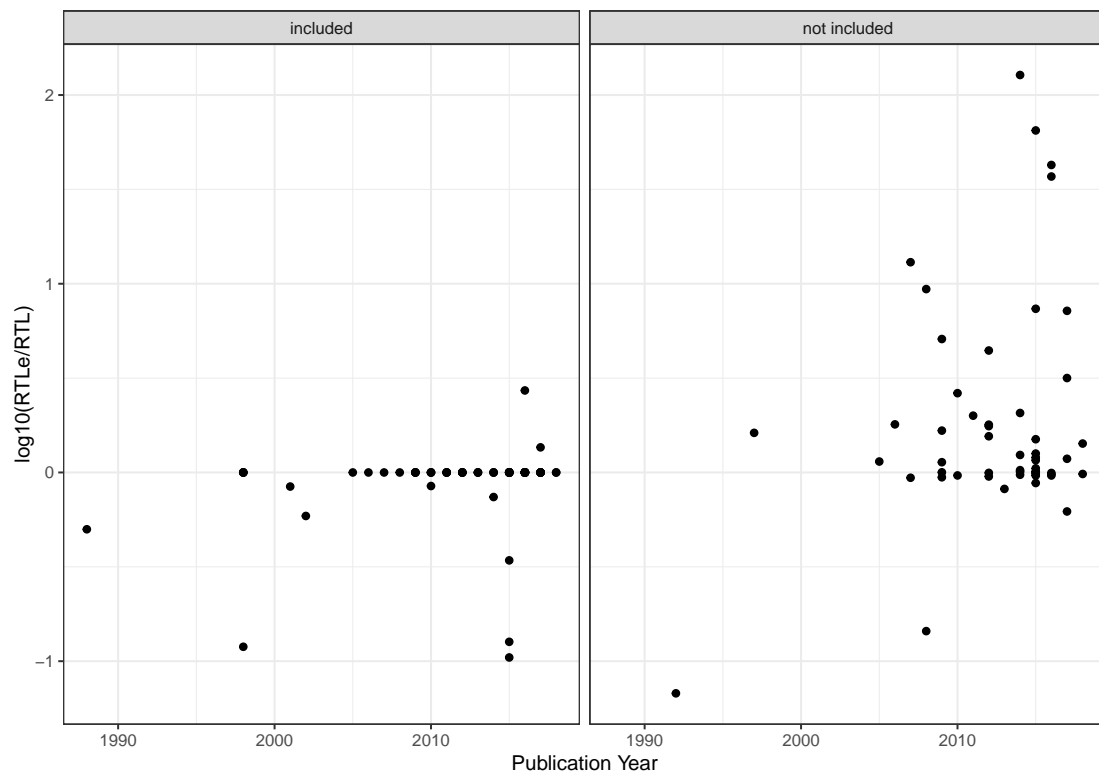


Figure A7. Comparison of model precision (expressed as \log_{10} ratio of RTLe to RTL) for ECOTOX database estimates in dependence on the publication year of the regulatory document for RTL that were included in the database and not included.

Appendix B. Evaluation of Aquatic Life Benchmarks (ALB)

In autumn 2018, it was tested whether ALB could be used for comprehensive risk evaluations instead of RTL, as they are provided by the US EPA, theoretically originate from the same sources as RTL (i.e., regulatory documents) and are also compiled by comparing effect endpoints with the respective level of concern [28]. Therefore, we tested whether the list of retrieved RTL for 143 pesticides agrees with the provided ALB for the same pesticides. It became apparent that for the 143 pesticides, approximately one third of ALB were either wrong or not included in this list (in October 2018). A recent check (October 2019) of the ALB revealed that the US EPA has updated the list of ALB. Thus, it was re-assessed whether the incorrect or outdated ALB were corrected, which was the case for 10 of the 143 reviewed pesticides. Still, after the most recent update, for a total of 25% of the evaluated pesticides, the ALB either deviate from the manually retrieved RTL from the most recent regulatory documents or no ALB is reported for the evaluated pesticides (n = 26 and 10 pesticides, respectively). Thus, the list of ALB, even though becoming more comprehensive, largely relies on regular updates. Additionally, a time lag between the publication and the most recent regulatory document and the referenced document in the ALB data collection became apparent (for wrong ALB, median time lag = 4 years, mean = 3.8 years). Finally, ALB were available for 486 unique pesticides (identified by CAS number), representing only a subsample of the actually reviewed active ingredients by the US EPA (i.e., 1140 published by July 2017 [30]).

References

- Oerke, E.C. Crop losses to pests. *J. Agric. Sci.* **2006**, *144*, 31–43. [CrossRef]
- Popp, J.; Pető, K.; Nagy, J. Pesticide productivity and food security. A review. *Agron. Sustain. Dev.* **2013**, *33*, 243–255. [CrossRef]
- Food and Agriculture Organization of the United Nations (FAO). FAO FAOSTAT Database. Available online: [http://www.fao.org/faostat/en/\\$\delimiter"026E30F\\$\#data/EL](http://www.fao.org/faostat/en/$\delimiter). (accessed on 1 November 2019).
- Bereswill, R.; Strelake, M.; Schulz, R. Current-use pesticides in stream water and suspended particles following runoff: Exposure, effects, and mitigation requirements. *Environ. Toxicol. Chem.* **2013**, *32*, 1254–1263. [CrossRef] [PubMed]
- Stone, W.W.; Gilliom, R.J.; Ryberg, K.R. Pesticides in U.S. Streams and Rivers: Occurrence and trends during 1992–2011. *Environ. Sci. Technol.* **2014**, *48*, 11025–11030. [CrossRef] [PubMed]
- Van Metre, P.C.; Alvarez, D.A.; Mahler, B.J.; Nowell, L.; Sandstrom, M.; Moran, P. Complex mixtures of Pesticides in Midwest US streams indicated by POCIS time-integrating samplers. *Environ. Pollut.* **2017**, *220*, 431–440. [CrossRef] [PubMed]
- FIFRA. *Federal Insecticide, Fungicide and Rodenticide act. U.S. Federal Law, Amended in 1972 and 1988*; FIFRA: Washington, DC, USA, 1947.
- U.S. Environmental Protection Agency. Reregistration and Other Review Programs Predating Pesticide Registration Review. Available online: <https://www.epa.gov/pesticide-reevaluation/reregistration-and-other-review-programs-predating-pesticide-registration> (accessed on 30 October 2019).
- U.S. Environmental Protection Agency. *Overview of the Ecological Risk Assessment Process in the Office of Pesticide Programs, US Environmental Protection Agency Endangered and Threatened Species Effects Determinations*; DIANE Publishing: Collingdale, PA, USA, 2004.
- U.S. Environmental Protection Agency. *Ecological Effects Test Guidelines OCSPP 850.1075: Freshwater and Saltwater Fish Acute Toxicity Test*; U.S. Environmental Protection Agency: Washington, DC, USA, 2016; pp. 1–19.
- U.S. Environmental Protection Agency. *Ecological Effects Test Guidelines OCSPP 850.1010: Aquatic Invertebrate Acute Toxicity Test, Freshwater Daphnids*; U.S. Environmental Protection Agency: Washington DC, USA, 2016; pp. 1–17.
- U.S. Environmental Protection Agency. *Ecological Effects Test Guidelines OCSPP 850.4400: Aquatic Plant Toxicity Test Using Lemna spp.*; U.S. Environmental Protection Agency: Washington, DC, USA, 2012; pp. 1–24.
- U.S. Environmental Protection Agency. *Ecological Effects Test Guidelines OCSPP 850.4500: Algal Toxicity*; U.S. Environmental Protection Agency: Washington, DC, USA, 2012; pp. 1–28.

14. US EPA Evaluation Guidelines for Ecological Toxicity Data in the Open Literature. Available online: <https://www.epa.gov/pesticide-science-and-assessing-pesticide-risks/evaluation-guidelines-ecological-toxicity-data-open> (accessed on 30 March 2018).
15. Wolfram, J.; Stehle, S.; Bub, S.; Petschick, L.L.; Schulz, R. Meta-analysis of insecticides in United States surface waters: Status and future implications. *Environ. Sci. Technol.* **2018**, *52*, 14452–14460. [[CrossRef](#)]
16. Stehle, S.; Schulz, R. Agricultural insecticides threaten surface waters at the global scale. *Proc. Natl. Acad. Sci. USA* **2015**, *112*, 5750–5755. [[CrossRef](#)] [[PubMed](#)]
17. Schulz, R.; Liess, M. A field study of the effects of agriculturally derived insecticide input on stream macroinvertebrate dynamics. *Aquat. Toxicol.* **1999**, *46*, 155–176. [[CrossRef](#)]
18. Schäfer, R.B.; Bundschuh, M.; Rouch, D.A.; Szöcs, E.; von der Ohe, P.C.; Pettigrove, V.; Schulz, R.; Nugegoda, D.; Kefford, B.J. Effects of pesticide toxicity, salinity and other environmental variables on selected ecosystem functions in streams and the relevance for ecosystem services. *Sci. Total Environ.* **2012**, *415*, 69–78. [[CrossRef](#)]
19. Schäfer, R.B.; Caquet, T.; Siimes, K.; Mueller, R.; Lagadic, L.; Liess, M. Effects of pesticides on community structure and ecosystem functions in agricultural streams of three biogeographical regions in Europe. *Sci. Total Environ.* **2007**, *382*, 272–285. [[CrossRef](#)]
20. Beketov, M.A.; Kefford, B.J.; Schäfer, R.B.; Liess, M. Pesticides reduce regional biodiversity of stream invertebrates. *Proc. Natl. Acad. Sci. USA* **2013**, *110*, 11039–11043. [[CrossRef](#)] [[PubMed](#)]
21. Schäfer, R.B.; Pettigrove, V.; Rose, G.; Allinson, G.; Wightwick, A.; von der Ohe, P.C.; Shimeta, J.; Kühne, R.; Kefford, B.J. Effects of pesticides monitored with three sampling methods in 24 sites on macroinvertebrates and microorganisms. *Environ. Sci. Technol.* **2011**, *45*, 1665–1672. [[CrossRef](#)] [[PubMed](#)]
22. Vijver, M.G.; Hunting, E.R.; Nederstigt, T.A.; Tamis, W.L.; van den Brink, P.J.; van Bodegom, P.M. Postregistration monitoring of pesticides is urgently required to protect ecosystems. *Environ. Toxicol. Chem.* **2017**, *36*, 860–865. [[CrossRef](#)] [[PubMed](#)]
23. Malaj, E.; Peter, C.; Grote, M.; Kühne, R.; Mondy, C.P.; Usseglio-Polatera, P.; Brack, W.; Schäfer, R.B. Organic chemicals jeopardize the health of freshwater ecosystems on the continental scale. *Proc. Natl. Acad. Sci. USA* **2014**, *111*, 9549–9554. [[CrossRef](#)]
24. Morrissey, C.A.; Mineau, P.; Devries, J.H.; Sanchez-Bayo, F.; Liess, M.; Cavallaro, M.C.; Liber, K. Neonicotinoid contamination of global surface waters and associated risk to aquatic invertebrates: A review. *Environ. Int.* **2015**, *74*, 291–303. [[CrossRef](#)]
25. Cairns, J. The myth of the most sensitive species. *BioScience* **1986**, *36*, 670–672. [[CrossRef](#)]
26. U.S. Environmental Protection Agency. Pesticides Chemical Search | Chemical Search | Pesticides | US EPA. Available online: <https://iaspub.epa.gov/apex/pesticides/f?p=chemicalsearch:1> (accessed on 2 March 2018).
27. U.S. Environmental Protection Agency. US EPA's Web Archive: Pesticide Reregistration Status. Available online: <https://archive.epa.gov/pesticides/reregistration/web/html/status.html> (accessed on 2 March 2018).
28. U.S. Environmental Protection Agency. Aquatic Life Benchmarks and Ecological Risk Assessments for Registered Pesticides. Available online: <https://www.epa.gov/pesticide-science-and-assessing-pesticide-risks/aquatic-life-benchmarks-and-ecological-risk> (accessed on 31 October 2019).
29. U.S. Environmental Protection Agency. *Special Docket for Pesticide Reregistration Risk Assessments-Risk Assessments and Related Documents (DVD Set)*; U.S. Environmental Protection Agency: Washington, DC, USA, 2007.
30. U.S. Environmental Protection Agency. Registration Review Process. Available online: <https://www.epa.gov/pesticide-reevaluation/registration-review-process> (accessed on 23 October 2019).
31. U.S. Environmental Protection Agency. (2019) ECOTOX User Guide: ECOTOXicology Knowledgebase System. Version 5.0. Available online: <http://www.epa.gov/ecotox/2019> (accessed on 1 November 2019).
32. U.S. Environmental Protection Agency. (2019) USEPA Pesticide Ecotoxicity Database. Available online: <https://ecotox.ipmcenters.org/index.cfm?menuid=7> (accessed on 1 November 2019).
33. U.S. Environmental Protection Agency. *Ecological Effects Test Guidelines OCSPP 850.1020: Gammarid Amphipod Acute Toxicity Test*; U.S. Environmental Protection Agency: Washington, DC, USA, 2016; pp. 1–18.
34. Beasley, A.; Belanger, S.E.; Otter, R.R. Stepwise Information-Filtering Tool (SIFT): A method for using risk assessment metadata in a nontraditional way: Stepwise Information-Filtering Tool (SIFT). *Environ. Toxicol. Chem.* **2015**, *34*, 1436–1442. [[CrossRef](#)]
35. Connors, K.A.; Beasley, A.; Barron, M.G.; Belanger, S.E.; Bonnell, M.; Brill, J.L.; de Zwart, D.; Kienzler, A.; Krailler, J.; Otter, R.; et al. Creation of a curated aquatic toxicology database: EnviroTox. *Environ. Toxicol. Chem.* **2019**, *38*, 1062–1073. [[CrossRef](#)]

36. Bub, S.; Wolfram, J.; Stehle, S.; Petschick, L.L.; Schulz, R. Graphing ecotoxicology: The MAGIC Graph for linking environmental data on chemicals. *Data* **2019**, *4*, 34. [[CrossRef](#)]
37. U.S. Environmental Protection Agency. *Environmental Fate and Ecological Risk Assessment Problem Formulation. In Support of Registration Review of Formetanate HCl*; U.S. Environmental Protection Agency: Washington, DC, USA, 2010.
38. R Core Team. *A Language and Environment for Statistical Computing*. Vienna, Austria: R Foundation for Statistical Computing; 2012; R Foundation for Statistical Computing: Vienna, Austria, 2019.
39. Wickham, H. *Ggplot2: Elegant Graphics for Data Analysis*; Springer: New York, NY, USA, 2009; ISBN 978-0-387-98140-6.
40. RPostgreSQL: R Interface to the 'PostgreSQL' Database System. Available online: <https://cran.r-project.org/web/packages/RPostgreSQL/index.html> (accessed on 1 November 2019).
41. WoRMS. *Editorial Board World Register of Marine Species*; WoRMS: Ostend, Belgium, 2019.
42. Stephen, C.E.; Mount, D.I.; Hansen, D.J.; Gentile, J.R.; Chapman, G.A.; Brungs, W.A. *Guidelines for Deriving Numerical National Water Quality Criteria for the Protection of Aquatic Organisms and Their Uses*; U.S. Environmental Protection Agency: Washington, DC, USA, 1985.
43. Guiry, M.D.; Guiry, G.M. *AlgaeBase*. World-Wide Electronic Publication, National University of Ireland, Galway. Available online: <https://www.algaebase.org> (accessed on 10 August 2019).
44. Pesticide Use in U.S. Crop Production: 2002. Available online: <https://pdfs.semanticscholar.org/739e/6ad4b29880c43ab7e8509e0af53111c69735.pdf> (accessed on 1 November 2019).
45. Haukoos, J.S.; Lewis, R.J. Advanced statistics: Bootstrapping confidence intervals for statistics with "difficult" distributions. *Acad. Emerg. Med.* **2005**, *12*, 360–365. [[CrossRef](#)]
46. Wood, M. Bootstrapped confidence intervals as an approach to statistical inference. *Organ. Res. Methods* **2005**, *8*, 454–470. [[CrossRef](#)]
47. Cumming, G. Inference by eye: Reading the overlap of independent confidence intervals. *Stat. Med.* **2009**, *28*, 205–220. [[CrossRef](#)] [[PubMed](#)]



© 2019 by the authors. Licensee MDPI, Basel, Switzerland. This article is an open access article distributed under the terms and conditions of the Creative Commons Attribution (CC BY) license (<http://creativecommons.org/licenses/by/4.0/>).

Video Recordings of Male Face and Neck Movements for Facial Recognition and Other Purposes

Collin Gros ¹ and Jeremy Straub ^{2,*}

¹ Department of Computer Science, Texas Tech University, Lubbock, TX 79409, USA

² Department of Computer Science, North Dakota State University, Fargo, ND 58108, USA

* Correspondence: jeremy.straub@ndsu.edu; Tel.: +1-701-231-8196

Received: 21 July 2019; Accepted: 3 September 2019; Published: 6 September 2019



Abstract: Facial recognition is made more difficult by unusual facial positions and movement. However, for many applications, the ability to accurately recognize moving subjects with movement-distorted facial features is required. This dataset includes videos of multiple subjects, taken under multiple lighting brightness and temperature conditions, which can be used to train and evaluate the performance of facial recognition systems.

Dataset: <https://doi.org/10.17632/xgg8xcscr5.1>; <https://doi.org/10.17632/f47pm7rwt3.1>

Dataset License: CC-BY

Keywords: facial recognition; males; video recordings; face and neck movement; human recognition

1. Summary

This dataset is comprised of video of multiple male subjects' head and shoulder areas while the subjects make regular movements, which can prospectively be used to train and test facial recognition algorithms. The subjects' movements are synchronized across the dataset to facilitate recognition time-based comparisons.

For each subject, data was collected for multiple head positions, light brightness and light temperature. The set of videos includes approximately 33,000 frames, recorded at a rate of 29.97 frames per second. Because these are not discrete images, but instead frames in a video, face detection, and identification during movement and recognition from video can also be assessed using this data.

To this end, the subjects' movements are synchronized between videos to facilitate comparison of algorithms based on total time subject is detected during the video. Specifically, the subjects move their head and neck through an entire range of motion. This facilitates the testing of recognition at different points using individual frames as well as the testing of algorithm performance on moving video data. This dataset can be used with large training sets otherwise available to test recognition with a large database of potential subjects to match to. The data was collected in a controlled environment with a consistent white background.

2. Background

Facial recognition has multiple uses including retail store [1,2], access control [3] and law enforcement [4] applications. Facial data can also help classify subjects by gender [5] and age [6] and provide insight into their current interest level and emotional state [7].

While much facial recognition research focuses on static images, many applications require the real-time or near-real-time identification of moving faces from video. Even if single video frames are used and presented to static facial recognition systems, they have movement blur and facial orientations

not supported by the static recognition system. For this reason, facial recognition from video, in many cases with static image training, is a key area of research.

Approaches which use support vector machines [8], tree-augmented naive-Bayes classifiers [9], AdaBoost [10], linear discriminant analysis [10], independent component analysis [11], Fisher linear discriminant analysis [11], sparse network of Winnows classifiers [12], k-nearest neighbor classifiers [12] and multiple other techniques [13] has been proposed. Some techniques have also been developed which take advantage of video properties [14] and motion history [12].

This dataset provides training and testing data for evaluating the performance of video facial recognition systems. In particular, it provides data for both static image and video-based training and video-based recognition. Subjects move their head to multiple positions, facilitating the comparison of algorithm performance with regards to subject head position. Additionally, data collected under different lighting brightness and temperature levels is included to facilitate the evaluation of lighting (as part of training or testing data sets) on algorithms.

3. Experimental Design, Materials, and Methods

This section discusses the equipment, configuration and experimental methods used to collect the dataset. First, the equipment and its configuration are discussed. Then the lighting conditions are presented. Finally, the experimental design is reviewed.

3.1. Equipment and Setup

A Sony AX100 4 K Expert Handycam (Tokyo, Japan) was used for video recording. The high definition 4 K videos (3840×2160 resolution at 29.97 frames per second) recorded were saved in the MP4 file format with the AVC codec. Two Neewer LED500LRC LED lights (Edison, NJ, USA) were used as background lighting. One Yongnuo YN600L LED light (Hot Springs, AK, USA) was used for the lighting of the subject. All lights and the camera were placed at stationary positions, depicted in Figure 1 with location measurements presented in Table 1. A Tekpower lumen meter (Montclair, CA, USA) was used to measure the lumens produced in each lighting configuration. A standard projector screen served as the backdrop for the photos. The audio present in the videos is the sound of an electronic metronome that indicates to the subject when it is time to change positions. This audio was recorded in stereo with a 48 kHz sampling rate using PCM encoding.

One lighting angle was used and the light was pointed directly towards the subject. The camera was placed in a fixed position near the light, also aimed at the subject.

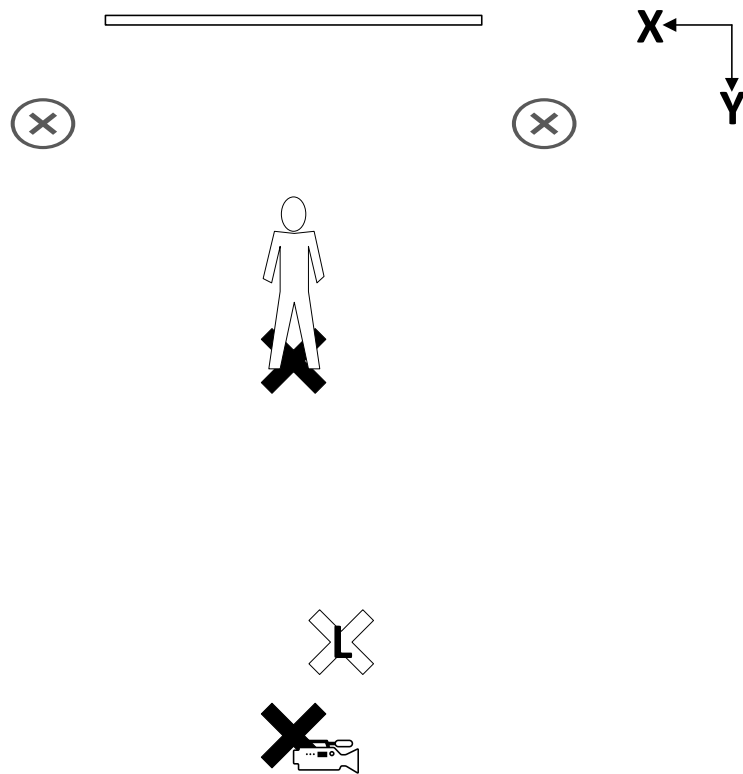


Figure 1. Depicts the positions of lights and the video camera.

Table 1. Camera, lights and subject positions.

Location	X Coordinate	Y Coordinate
Subject Light	84.5	127.5
Background 1	43.5	50.5
Background 2	129	47
Camcorder	97	132
Subject	96.5	63.5

3.2. Lighting

The subject was filmed under multiple lighting levels, which are summarized in Table 2. The lighting of the subject from the Yongnuo YN600L LED light was set at 60% brightness on warm (3200 k), 60% brightness on cold (5500 k), 10% brightness on warm (3200 k) with 10% brightness on cold (5500 k), 40% brightness on warm (3200 k) with 40% brightness on cold (5500 k), and 70% brightness on warm (3200 k) with 70% brightness on cold (5500 k). Lumen readings were measured using a Tekpower lumen meter and these values are also included in Table 2.

Table 2. Light setting equipment configuration and measurements of lumens produced for each light setting.

Configuration	Light Settings	Lumens
Warm	60% brightness on warm (3200 k)	280
Cold	60% brightness on cold (5500 k)	391
Low	10% brightness on warm (3200 k) and 10% brightness on cold (5500 k)	155
Medium	40% brightness on warm (3200 k) and 40% on brightness on cold (5500 k)	492
High	70% brightness on warm (3200 k) and 70% brightness on cold (5500 k)	745

3.3. Subjects & Procedure

Five videos were taken for each of 11 subjects, using a protocol approved by the NDSU institutional review board, for a total of 55 videos. The subjects were males between the ages of 18 and 26. A few of the subjects had small beards, while the rest have minimal facial hair.

Each of the five videos, for each subject, uses a different lighting configuration. These lighting configurations are depicted in Figure 2. The videos are approximately 20 s long and the subject moves his head to a new standardized position every second. Markers were placed on the walls, floor, and ceilings that the subjects were instructed to look at, to correctly position their heads.



Figure 2. The different lighting settings used for each video (left to right: Warm, Cold, Low, Medium, and High).

The subject was told to move their head after immediately upon hearing a metronome-like clicking sound. The time between each tick was one second. Because of this, each subject spends approximately the same amount of time facing in each position and moving between positions. This allows the impact of the lighting conditions on different facial recognition algorithms to be compared in terms of aggregate face detection time, as each view of the subject's face was visible for the approximately the same amount of time in each video. Figure 3 depicts the various positions each subject positioned his head in.



Figure 3. Subjects were told to position their head in multiple orientations, for one second at a time, during video recording.

4. Comparison to Other Data Sets

A number of data sets exist that have been collected for performing facial recognition work. The majority of these data sets are collections of individual images. Commonly used data sets range in size from the "ORL Database of Faces" which has 400 images for 10 individuals [15] to the "MS-Celeb-1M" dataset which has 10,000,000 images for 100,000 people [16]. Data sets also vary in the number of images that are presented for each subject. The "Labeled Faces in the Wild" data set, for example, included only two images per individual [17]. The "Pgu-Face" dataset had 4 images per individual [18] and the "FRGC 1.0.4" dataset had approximately 5 images per person [19]. Other data sets, such as the "IARPA Janus Benchmark A" [20] and "Extended Cohn-Kanade Dataset (CK+)" [21] have a larger number, including 11.4 and 23 images per individual, respectively. Prior work included producing data sets with 525 [22] and 735 [23] images per subject.

The dataset described herein is comprised of 55 videos (of 11 subjects) which are each approximately 20 seconds in length. Recorded at 29.97 frames per second, this means that each video is approximately 600 frames and that there are approximately 3,000 frames of each subject and 33,000 frames, in total,

for all 11 subjects. This places this dataset towards the larger end of the spectrum, in terms of the total number of frames or images.

Data sets have been collected in a variety of ways. Learned-Miller, et al. [17] created a dataset entitled “Labeled Faces in the Wild” which included 13,000 images for 5,749 people. This data set was harvested from websites. Guo, et al. [16] also created a harvested dataset, “MS-Celeb-1M” of 10,000,000 images covering 100,000 people. Many other datasets are manually collected using volunteer subjects. These databases are typically smaller with images of fewer individuals. The “ORL Database of Faces” contained images of 10 people [15]. Larger datasets included the Georgia Tech Face Database with images of 50 people [24] and the AR Face Database [25] with images of 126 individuals.

Most manually collected datasets present multiple views of the subject, in many cases from different angles. In some cases, lighting or other environmental conditions are varied. The “Extended Yale Face Database B” [26], for example, included 9 poses and 64 lighting settings per subject. In other cases (such as the “Pgu-Face” dataset [18]), objects are placed in front of the subjects to facilitate the testing of the recognition of partially occluded faces. In prior work [22,23], subjects were imaged from multiple camera perspectives and with lighting in different positions and at different levels of brightness and at different temperatures.

The dataset described herein includes multiple lighting levels; however, the subject is asked to reposition his head into multiple positions (shown in Figure 3) instead of changing the position of the camera, the lighting location or other variables. In addition, this dataset includes continuous recordings of videos of subjects’ movement, allowing assessment of recognition in the fixed positions as well as in intermediate positions.

A final aspect of datasets that should be compared is their resolution. Datasets vary significantly in this regard, ranging from smaller images such as the Georgia Tech database (with a resolution of 640×640 pixels) [24] to multi-megapixel images (such as those presented in [22,23]). The 4 K video files presented in this dataset have a resolution of 3840×2160 pixels.

Author Contributions: Conceptualization, C.G. and J.S.; data curation, C.G.; writing—original draft preparation, C.G. and J.S.; writing—review and editing, J.S.; supervision, J.S.; project administration, J.S.; funding acquisition, J.S.

Funding: The collection of this data was supported by the United States National Science Foundation (NSF award # 1757659).

Acknowledgments: Thanks is given to William Clemons and Marco Colasito who aided in the collection of this data. Facilities and some equipment used for the collection of this data were provided by the North Dakota State University Institute for Cyber Security Education and Research and the North Dakota State University Department of Computer Science.

Conflicts of Interest: The authors declare no conflict of interest. The funders had no role in the design of the study; in the collection, analyses, or interpretation of data; in the writing of the manuscript, or in the decision to publish the results.

References

- Denimarck, P.; Bellis, D.; McAllister, C. Biometric System and Method for Identifying a Customer upon Entering a Retail Establishment. U.S. Patent Application No. US2003/0018522 A1, 23 January 2003.
- Lu, D.; Kiewit, D.A.; Zhang, J. Market Research Method and System for Collecting Retail Store and Shopper Market Research Data. U.S. Patent US005331544A, 19 July 1994.
- Kail, K.J.; Williams, C.B.; Kail Richard, L. Access Control System with RFID and Biometric Facial Recognition. U.S. Patent Application No. US2007/0252001 A1, 1 November 2007.
- Introna, L.; Wood, D. Picturing algorithmic surveillance: The politics of facial recognition systems. *Surveill. Soc.* **2004**, *2*, 177–198. [[CrossRef](#)]
- Wiskott, L.; Fellous, J.-M.; Krüger, N.; von der Malsburg, C. Face Recognition and Gender Determination. In Proceedings of the International Workshop on Automatic Face and Gesture Recognition, Zurich, Switzerland, 26–28 June 1995; pp. 92–97.
- Ramesha, K.; Raja, K.B.; Venugopal, K.R.; Patnaik, L.M. Feature Extraction based Face Recognition, Gender and Age Classification. *Int. J. Comput. Sci. Eng.* **2010**, *2*, 14–23.

7. Yeasin, M.; Sharma, R.; Yeasin, M.; Member, S.; Bulot, B. Recognition of facial expressions and measurement of levels of interest from video. *IEEE Trans. Multimed.* **2006**, *8*, 500–508. [CrossRef]
8. Michel, P.; El Kaliouby, R. Real time facial expression recognition in video using support vector machines. In Proceedings of the 5th International Conference on Multimodal Interfaces-ICMI '03, Vancouver, BC, Canada, 5–7 November 2003; ACM Press: New York, NY, USA, 2003; p. 258.
9. Cohen, I.; Sebe, N.; Garg, A.; Lew, M.S.; Huang, T.S. Facial expression recognition from video sequences. In Proceedings of the IEEE International Conference on Multimedia and Expo, Lausanne, Switzerland, 26–29 August 2002; pp. 121–124.
10. Littlewort, G.; Bartlett, M.S.; Fasel, I.; Susskind, J.; Movellan, J. Dynamics of facial expression extracted automatically from video. *Image Vis. Comput.* **2006**, *24*, 615–625. [CrossRef]
11. Uddin, M.; Lee, J.; Kim, T.-S. An enhanced independent component-based human facial expression recognition from video. *IEEE Trans. Consum. Electron.* **2009**, *55*, 2216–2224. [CrossRef]
12. Valstar, M.; Pantic, M.; Patras, I. Motion history for facial action detection in video. In Proceedings of the IEEE International Conference on Systems, Man and Cybernetics—Cover (IEEE Cat. No.04CH37583), The Hague, The Netherlands, 10–13 October 2004; pp. 635–640.
13. Matta, F.; Dugelay, J.-L. Person recognition using facial video information: A state of the art. *J. Vis. Lang. Comput.* **2009**, *20*, 180–187. [CrossRef]
14. Gorodnichy, D.O. Facial Recognition in Video. In *Audio- and Video-Based Biometric Person Authentication*, 1st ed.; Springer: Berlin/Heidelberg, Germany, 2003; pp. 505–514.
15. The Database of Faces. Available online: <https://www.cl.cam.ac.uk/research/dtg/attarchive/facedatabase.html> (accessed on 29 January 2019).
16. Guo, Y.; Zhang, L.; Hu, Y.; He, X.; Gao, J. MS-Celeb-1M: A Dataset and Benchmark for Large-Scale Face Recognition. *arXiv*. 2016. Available online: <https://arxiv.org/abs/1607.08221> (accessed on 15 July 2019).
17. Learned-Miller, E.; Huang, G.B.; RoyChowdhury, A.; Li, H.; Hua, G. Labeled Faces in the Wild: A Survey. In *Advances in Face Detection and Facial Image Analysis*; Kawulok, M., Celebi, M.E., Eds.; Springer: Basel, Switzerland, 2016.
18. Salari, S.R.; Rostami, H. Pgu-Face: A dataset of partially covered facial images. *Data Brief* **2016**, *9*, 288–291. [CrossRef]
19. Ahonen, T.; Rahtu, E.; Ojansivu, V.; Heikkila, J. Recognition of blurred faces using Local Phase Quantization. In Proceedings of the 19th International Conference on Pattern Recognition, Tampa, FL, USA, 8–11 December 2008; pp. 1–4.
20. Klare, B.; Klein, B.; Taborsky, E.; Blanton, A.; Cheney, J.; Allen, K.E.; Grother, P.; Mah, A.; Jain, A.K.; Burge, M.; et al. Pushing the Frontiers of Unconstrained Face Detection and Recognition: IARPA Janus Benchmark A. In Proceedings of the Computer Vision and Pattern Recognition Conference, Boston, MA, USA, 7–12 June 2015; pp. 1931–1939.
21. Lucey, P.; Cohn, J.F.; Kanade, T.; Saragih, J.; Ambadar, Z.; Matthews, I. The Extended Cohn-Kanade Dataset (CK+): A complete dataset for action unit and emotion-specified expression. In Proceedings of the 2010 IEEE Computer Society Conference on Computer Vision and Pattern Recognition-Workshops, San Francisco, CA, USA, 13–18 June 2010; pp. 94–101.
22. Gros, C.; Straub, J. Human face images from multiple perspectives with lighting from multiple directions with no occlusion, glasses and hat. *Data Brief* **2018**, *22*, 522–529. [CrossRef]
23. Gros, C.; Straub, J. A Dataset for Comparing Mirrored and Non-Mirrored Male Bust Images for Facial Recognition. *Data* **2019**, *4*, 26. [CrossRef]
24. Nefian, A.V. Georgia Tech Face Database. Available online: http://www.anejian.com/research/face_reco.htm (accessed on 15 July 2019).
25. Martinez, A.M. AR Face Database Webpage. Available online: <http://www2.ece.ohio-state.edu/~jaleix/ARdatabase.html> (accessed on 22 August 2019).
26. Georgiades, A.S.; Belhumeur, P.N.; Kriegman, D.J. From few to many: Illumination cone models for face recognition under variable lighting and pose. *IEEE Trans. Pattern Anal. Mach. Intell.* **2001**, *23*, 643–660. [CrossRef]



Data Descriptor

Dataset on Substrate-Borne Vibrations of *Constrictotermes cyphergaster* (Blattodea: Isoptera) Termites

Lívia Fonseca Nunes ^{1,*}, Paulo Fellipe Cristaldo ², Pedro Sérgio Silva ³,
Leonardo Bonato Felix ³, Danilo Miranda Ribeiro ¹ and Og DeSouza ^{1,*}

¹ Department of Entomology, Federal University of Viçosa, Viçosa, MG 36570-900, Brazil; dmrib.cs@gmail.com

² Department of Agronomy, Federal Rural University of Pernambuco, Recife, PE 52171-900, Brazil; pfellipec@gmail.com

³ Department of Electrical Engineering, Federal University of Viçosa, Viçosa, MG 36570-900, Brazil; pedrosergiot@gmail.com (P.S.S.); leobonato@ufv.br (L.B.F.)

* Correspondence: livfnunes@gmail.com (L.F.N.); og.souza@ufv.br (O.D.);
Tel.: +55-3138994017 (L.F.N.); +55-3138994004 (O.D.)

Received: 24 May 2019; Accepted: 18 June 2019; Published: 19 June 2019



Abstract: Here we present data on distinct stimuli as elicitors of substrate-borne vibrations performed by groups of termites belonging to the species *Constrictotermes cyphergaster* (Blattodea: Isoptera: Termitidae: Nasutitermitinae). The study consisted of assays where termite workers and soldiers were exposed to different airborne stimuli and the vibrations thereby elicited were captured by an accelerometer attached under the floor of the arena in which the termites were confined. A video camera was also used as a visual complement. The data provided here contribute to fill a gap currently existing in published datasets on termite communication.

Dataset: 10.5281/zenodo.2790686.

Dataset License: CC-BY 4.0

Keywords: termite vibrational reaction; stimuli; soldier's head extract

1. Summary

Vibration signaling is widespread in insects [1]. Such a communication channel can be used in a range of situations, e.g., to detect predators [2], prey [3], mates [4], and to recruit nestmates [5]. Furthermore, vibration can also be used as an important component to establish communication with another individual or a group of individuals.

Termites are social insects that are well known to use vibrations to convey information to their nestmates or to gather contextual information about the environment. For instance, by combining substrate-borne vibrations with chemical scents, termites communicate alarm [6]. They are also able to use the resonant frequency of a block of wood to assess its size, thereby choosing one food item over another [7]. Termites are also sensitive to heterospecific vibration, using that information for their own benefit: as recently demonstrated [8], termites can escape danger by eavesdropping the vibrational cues emitted by predatory ants. In spite of such an importance, vibratory communication in termites is relatively underexplored, and published datasets on the subject are definitely very rare.

To cover such a gap, here we present a large dataset (c.a. 13 million lines) containing the intensity of the substrate-borne vibration of termite groups confined in arenas specially designed to amplify

such vibrations (see [9]). Vibrations were measured using an accelerometer and were triggered by airborne stimuli.

2. Data Descriptor

Here we provide the raw data describing the intensity of substrate-borne vibrations produced by groups of termites confined in arenas bearing a flexible floor. Such arenas (Figure 1; so-called “tympanic” in allusion to their flexible floor) were designed to amplify the feeble vibrations produced by the termites and are fully described and tested by Nunes et al. [9]. Vibrations were measured by an accelerometer whose sensor was attached to the outer surface of the arenas’ floor.

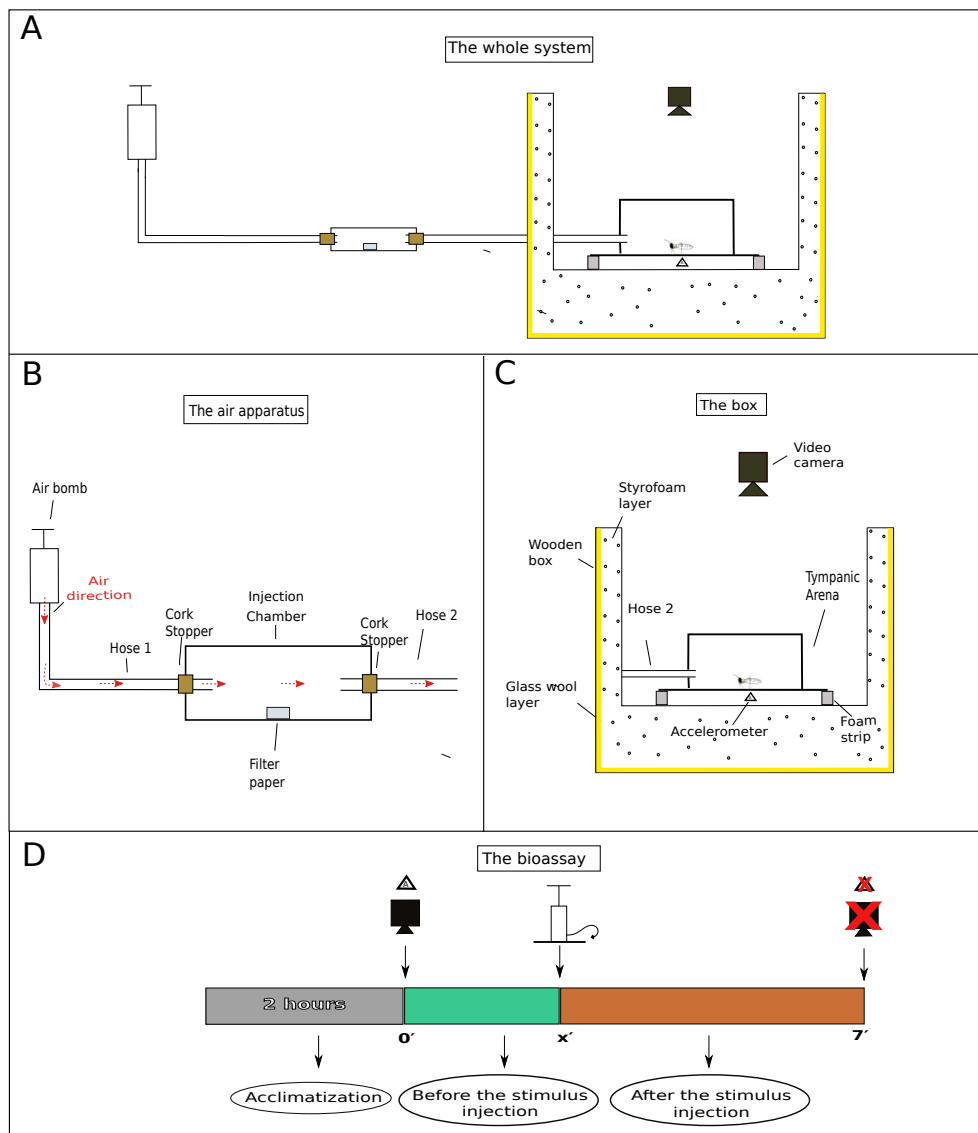


Figure 1. Schematic depiction of the setup designed to measure termite vibrational responses when subjected to different stimuli. (A) Global view of the setup, showing an air pump connected by hoses through a injection chamber and to a tympanic arena housed in a wooden box. (B) Detailed view of the air pumping system, showing the injection chamber used to house the sources of stimuli. (C) Detailed view of the wooden box lined with styrofoam and glass wool to minimize external noise disturbance. (D) The chronology of each assay: (i) each termite group was allowed at least 2 h of acclimatization before the beginning of the assays; (ii) video and accelerometer recordings start about 2 min before the stimulus injection; (iii) after injecting the stimulus, recordings proceed for another 5 min, totaling 7 min of readings. “x” is the exactly time at which the stimulus was injected, which is given in Table 1.

Each termite group was composed of 12 workers and 3 soldiers from a given nest. Vibrations were triggered by subjecting these termites to distinct airborne stimuli gently pumped into the arena after termites were allowed to acclimatize for 2 h.

Readings thereby produced are presented here in a series of comma-separated values (.csv) files. Each file corresponds to a full assay on a single termite group from a single nest and with a single stimulus. Each line in the file presents the readings of termite vibrations captured by the accelerometer at the “x” (horizontal), “y” (horizontal), and “z” (vertical) axes (Figure 2) at a given time. The accelerometer was configured at high gain. Readings are expressed in “counts” units. There are 13,108 counts per g (the acceleration due to gravity) in high gain mode. Each set of 512 lines corresponds to 1 s (more details are given in Section 3.5).

The columns in the datafiles are:

- time:** the moment, from the beginning of the recording session, when vibration was recorded
- Ax:** counts read by the accelerometer at the horizontal x axis
- Ay:** counts read by the accelerometer at the horizontal y axis
- Az:** counts read by the accelerometer at the vertical z axis
- NestID:** the field identification of the nest from which the termite group was collected. Codes within NestID column are built as nnncccyyy, where nnn = the nest sequential number used as a field label; ccc = the initials of the collector (name and surname); yyy = the year in which the nest was taken from the field to the lab.
- TypeStimulus:** the type of stimulus that was deposited within the injection chamber to be carried by the air injected into the arena to trigger termite vibrations. Codes within TypeStimulus are: air = only air; air_paper = air plus a piece of filter paper was deposited into the injection chamber and the air therein was injected into the arena; air_paper_hexane = a piece of filter paper onto which hexane was applied was deposited into the injection chamber and the air therein was injected into the arena; air_paper_extract = a piece of filter paper onto which a hexane extract from soldiers’ heads was applied was deposited into the injection chamber and the air therein was injected into the arena.
- TermiteGroup:** the identification of the nest from which the termite group was collected and the stimulus they were exposed to. Codes within the TermiteGroup column are built as gnns, where: g = “group”; nn = the nest sequential number at which the termite group was collected; s = the stimulus that the termite group was exposed to.

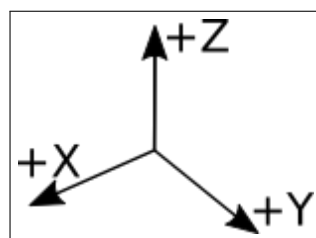


Figure 2. The orientation of the X, Y, and Z axes from which vibrations were captured by the accelerometer.

3. Methods

3.1. Ethical Statement

The current study is in compliance with the relevant regulations of Brazil, including collection and transportation permits from The Brazilian Institute for the Environment and Renewable Natural Resources (IBAMA), and permission from The Brazilian Enterprise for Agricultural Research (EMBRAPA, CNPMS) to conduct the study on their site. O. DeSouza holds a permanent collecting and transporting permit (# 10014-1) from IBAMA. Tacit approval from the Brazilian Government is implied by the authors being hired as scientific researchers. The species collected for the present

study are neither endangered nor protected, and thus no specific permits were required for laboratory experiments. No genetic information was accessed.

3.2. Termite Material

Assays were conducted using termites from 15 wild colonies of *C. cyphergaster* (Silvestri, 1901) collected in April 2017 in the Brazilian “cerrado”, near the town of Sete Lagoas (27°19' S, 14°44' W; altitude 800–900 m above sea level), Minas Gerais State, Southeastern Brazil. The colonies were transported to Viçosa (Minas Gerais, Brazil), where they were kept in laboratory in room-level conditions of humidity, temperature, and light. As food, the bark of trumpet trees (*Tabebuia aurea*, Bignoniaceae) was offered ad libitum to all nests. Water was also offered ad libitum through a piece of cotton attached to the opening of a test tube full of water.

3.3. Experimental Procedures

The assays were conducted from April to mid-July 2017. They were designed to measure the vibrational reaction exhibited by workers and soldiers of *C. cyphergaster* when they are subjected to different stimuli.

To perform the assays, we designed an experimental setup to minimize noise and vibrations from human traffic and other activities in nearby labs (Figure 1A). This setup consisted of a wooden box lined with (approx.) a 5-cm thick layer of glass wool plus an 8-cm thick styrofoam layer.

In order to amplify the feeble vibrations exhibited by the termites, we used an arena bearing a flexible floor (so as to mimic a tympanum) as described and tested by Nunes et al. [9]. The tympanic arena was placed inside the wooden box described above, over a pair of egg crate foam strips lying on a hollowed, cubic styrofoam structure (Figure 1C). Groups of 15 termite individuals (12 workers + 3 soldiers) were taken from their colonies and placed inside the arena (one group at a time). At least 2 h were allowed for termites to acclimatize before the beginning of the assays. The number of termites and caste ratio of the groups were chosen according to natural proportions found in field nests (4.5 workers: 1 soldier) [10] and within the range of densities known to improve interindividual interactions and survival [11].

Stimuli were offered to termites by gently pumping air through a hose to an injection chamber and from there through another hose to the arena (Figure 1A). This injection chamber (internal space: \varnothing 18 mm \times 80 mm long) was used to house any source of stimulus in addition to air (Figure 1B). Both ends of the injection chamber were sealed with cork stoppers. A small hole was made in the cork stoppers to connect the ends of the two hoses (\varnothing = 4 mm). The other end of the first hose (Figure 1B, hose 1; \approx 1190 mm long) was coupled to an air pump and the end of the other hose (Figure 1B, hose 2; \approx 650 mm long), which flowed directly into the tympanic arena. A light touch was given to the air pump lever, which descended by weight and gravity, blowing the stimulus from the injection chamber to the arena where the individuals were confined (Figure 1C). A total of c.a. 230 cm³ of air was injected into the system by the air pump.

The stimuli consisted of injecting into the arena:

1. the air present in the injection chamber;
2. the air present in the injection chamber after it had contact with a piece of filter paper (7 \times 2 cm) previously deposited therein;
3. the air present in the injection chamber after it had contact with a known amount of hexane that was loaded onto a piece of filter paper deposited in the injection chamber;
4. the air present in the injection chamber after it had contact with hexane extracts of termite soldier heads. These extracts were loaded onto a piece of filter paper deposited in the injection chamber.

Each assay was recorded on video and registered by the accelerometer for a total of 7 min divided into “time before the stimulus injection” and “time after the stimulus injection” (Figure 1D). This was

done to differentiate the activity of the groups before the stimulus injection from the activity after the stimulus injection, in order to obtain only the real effect of each stimulus on the termites' behavior.

Due to operational reasons, both the time of the stimulus injection and the volume of stimulus applied onto the filter paper varied among assays. These are specified in Table 1. Each nest provided four termite groups to be independently assayed with a given stimulus. Each group was assayed only once.

Table 1. Overview of stimuli at which termites were exposed to. Nest—the identification of the nest from which the termite group was collected. The nest identity code followed the sequence “nnncccyyy”, where *nnn* = nest sequential number used as field label; *ccc* = initials of collector (name and surname); *yyy* = year in which the nest was taken from the field to the lab. Stimulus—the kind of stimulus applied to each termite group, where “A” is air; “AP” is air + filter paper; “APH” is air + paper + hexane, and “APE” is air + paper + extract. Injection time—the time (s) at which the stimulus was injected. Aliquot applied—the proportional volume of hexane or extract applied at each assay. Head equivalence—how many heads of soldiers the aliquot corresponds to. Missing values are indicated by a dash.

Nest	Stimulus	Injection Time (s)	Aliquot Applied (μ L)	Head Equivalence
N01YCC2017	A	120	0.00	0
	AP	120	0.00	0
	APH	120	3.26	0
	APE	120	3.26	1
N02YCC2017	A	122	0.00	0
	AP	120	0.00	0
	APH	120	6.69	0
	APE	122	6.69	3
N03YCC2017	A	120	0.00	0
	AP	120	0.00	0
	APH	120	13.5	0
	APE	140	13.5	5
N04YCC2017	A	129	0.00	0
	AP	120	0.00	0
	APH	125	24.68	0
	APE	123	24.68	7
N05YCC2017	A	123	0.00	0
	AP	–	–	–
	APH	120	47.57	0
	APE	123	47.57	9
N06YCC2017	A	122	0.00	0
	AP	120	0.00	0
	APH	120	4.61	0
	APE	120	4.61	1
N07YCC2017	A	122	0.00	0
	AP	144	0.00	0
	APH	120	11.98	0
	APE	120	11.98	3
N08YCC2017	A	122	0.00	0
	AP	120	0.00	0
	APH	120	28.9	0
	APE	180	28.9	5
N09YCC2017	A	120	0.00	0
	AP	120	0.00	0
	APH	120	25.2	0
	APE	123	25.2	7

Table 1. Cont.

Nest	Stimulus	Injection Time (s)	Aliquot Applied (μL)	Head Equivalence
N10YCC2017	A	120	0.00	0
	AP	–	–	–
	APH	126	49.32	0
	APE	122	49.32	9
N11YCC2017	A	120	0.00	0
	AP	120	0.00	0
	APH	120	1.6	0
	APE	120	1.6	1
N12YCC2017	A	120	0.00	0
	AP	120	0.00	0
	APH	122	15.54	0
	APE	120	15.54	3
N13YCC2017	A	120	0.00	0
	AP	120	0.00	0
	APH	120	24.5	0
	APE	120	24.5	5
N14YCC2017	A	120	0.00	0
	AP	120	0.00	0
	APH	113	20.79	0
	APE	141	20.79	7
N15YCC2017	A	120	0.00	0
	AP	120	0.00	0
	APH	141	45.36	0
	APE	120	45.36	9

3.4. Extract Preparation

The soldiers of phylogenetic advanced termites species have a secretory epithelium located inside a large sac in their head known as a frontal gland. This gland is responsible for the production of a blend of chemicals that is related to alarm situations [12,13]. In *C. cyphergaster*, such chemicals are composed of (1S)- α -pinene, myrcene, and (E)- β -ocimene [6], which are known to be soluble in hexane. To provide assayed termites with this type of stimulus, we prepared hexane extracts from soldiers' heads, following Cristaldo et al., 2015 [6], as described below and depicted in Figure 3.

A total of 20 soldiers were taken from their respective nest and anesthetized on ice to have their heads severed and cut so as to expose the frontal gland. The heads were then immersed in hexane (10 μL per head) and left for 24 h in a freezer at ≈ 2.4 °C, after which the resulting extract was separated from the termite heads with the help of a microsyringe and again stored in the freezer at ≈ 2.4 °C until used in the assays. From each termite nest, we prepared only one extract.

Because termite heads vary in the amount of hexane they absorb, each termite group from a given nest produced a distinct initial volume of extract. For each nest, a given aliquot of extract would thus represent a particular amount of termite heads. Due to this, we kept track of the precise volume of extract offered to termites in a given assay so that we could know how many “head equivalents” this volume represented. For comparability, this same volume was used in the assays using only hexane. The volumes used in each assay, as well as their head equivalences, are listed in Table 1.

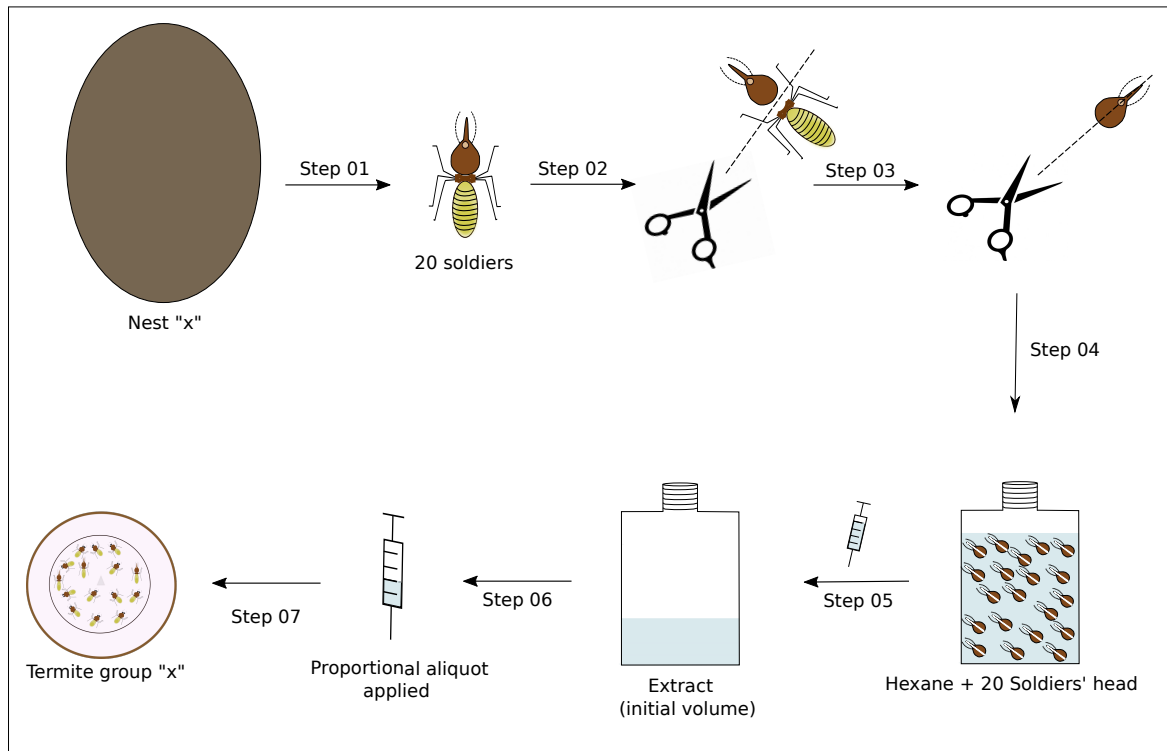


Figure 3. Overview of steps used to prepare the soldiers' head extracts. *Step 01:* 20 termites soldiers were taken from their respective colonies; *Step 02:* the soldiers were anesthetized on ice and dissected into the head and rest of body; *Step 03:* the soldiers' heads were cut from the base of the neck to the nasus; *Step 04:* the heads were placed into hexane (10 μ L per head) for 24 h at ≈ 2.4 $^{\circ}$ C; *Step 05:* the resulting extract was separated from the termite heads with the help of a microsyringe; *Step 06:* a known aliquot of this extract was collected from its initial volume, the aliquot being proportional to the amount of soldier heads we wanted to apply; *Step 07:* the aliquot was offered to a given termite group in a given assay. Assays are detailed in Table 1.

3.5. Behavioral Response and Parameters Measured

Substrate-borne vibrations produced by the assayed termites were recorded using a USB accelerometer (Gulf Coast Data Concepts, LLCTM model X2-2 logger) equipped with a Kionix KXRB5-2050TM sensor at 2.5 volts, which results in a sensitivity factor of 500 mv/g. These electrical stimuli are recorded by the accelerometer independently in three axes (x, y, and z, Figure 2) as "counts". The number of counts is recorded 512 times in each second. Therefore, each line in the files produced by the accelerometer (henceforth referred to as a "reading") contains the number of counts read in $1/512$ s. These files form the basis on which we have built the datafile here presented (Section 2). To convert these counts into g (gravity acceleration), it suffices to divide the number of counts by 13,108 because this is a correcting factor corresponding to the high gain mode in which we operated the accelerometer (Section 2). To facilitate the assay, the sensor was removed from the accelerometer's case while keeping it connected to the recording unit by electric wires. In doing so, we could attach this sensor directly to the external bottom surface of the arenas. This setup allowed us to record a series of 215,040 readings (512 readings \times 60 s \times 7 min) per assayed termite group, totaling about 12,840,000 readings = (215,040 readings \times 4 stimuli \times 15 assays) – (2 missing assays \times 215,040 readings) for the whole experiment. As a visual complement, we also recorded the termite group's activity in each assay using a SONY HDR-CX405TM digital video camera set to record 30 frames per second at Full HD (1920 \times 1080 60p). The camera positioning and the chronology of this footage are explained in detail in Figure 1.

Author Contributions: “Conceptualization”: L.F.N., O.D. and P.F.C.; “Data curation”: D.M.R., L.F.N. and O.D.; “Funding acquisition”: L.F.N. and O.D.; “Investigation”: L.F.N. and O.D.; “Methodology”: L.F.N., O.D., D.M.R., L.B.F. and P.S.S.; “Project administration”: L.F.N.; “Resources”: L.F.N. and O.D.; “Supervision”: L.F.N. and O.D.; “Validation”: L.F.N., O.D. and P.F.C.; “Visualization”: L.F.N., O.D., D.M.R., L.B.F. and P.S.S.; “Writing—original draft”: L.F.N. and O.D.; “Writing—review & editing”: L.F.N., O.D., D.M.R., L.B.F. and P.S.S.

Funding: This work was supported by the Brazilian Council for Research (CNPq), Minas Gerais State Agency for Research Support (FAPEMIG), and Coordination for the Improvement of Higher Education Personnel (CAPES). ODS holds a CNPq fellowship (# 307990/2017-6).

Acknowledgments: Many thanks to Octavio Miramontes (Institute of Physics—UNAM, Mexico) for providing the accelerometer and to Alex Koone (Gulf Coast Data Concepts engineer) who made the necessary modifications to the accelerometer for the study. We also thank Sidney G. Alves (Department of Physics and Mathematics at UFSJ) who came up with the idea of using an embroidery hoop as a tympanum. Our thanks also go to Ivan Cruz and Fernando Valicente from EMPRAPA-CNPMS for logistics support. This work was carried out using free software, especially, but not restricted to, L^AT_EX+ kyle, Ubuntu + Debian, Inkscape, Libreoffice, JabRef, Chrome, and custom-bib, as well as the free searching site Google Scholar, to which we are profoundly thankful. This is contribution no. 78 from the Termitology Laboratory at UFV, Brazil (<http://www.isoptera.ufv.br>) and derives from LFN’s MSc thesis defended at the UFV Graduate Program in Entomology (<http://www.pos.entomologia.ufv.br>).

Conflicts of Interest: The authors declare no conflict of interest.

References

- Hill, P.S. Vibration and animal communication: A review. *Am. Zool.* **2001**, *41*, 1135–1142. [[CrossRef](#)]
- Castellanos, I.; Barbosa, P. Evaluation of predation risk by a caterpillar using substrate-borne vibrations. *Anim. Behav.* **2006**, *72*, 461–469. [[CrossRef](#)]
- Fertin, A.; Casas, J. Orientation towards prey in antlions: Efficient use of wave propagation in sand. *J. Exp. Biol.* **2007**, *210*, 3337–3343. [[CrossRef](#)] [[PubMed](#)]
- Goulson, D.; Birch, M.C.; Wyatt, T.D. Mate location in the deathwatch beetle, *Xestobium Rufovillosum* De Geer (Anobiidae): Orientat. Substrate Vib. *Anim. Behav.* **1994**, *47*, 899–907. [[CrossRef](#)]
- Schneider, S.S.; Stamps, J.A.; Gary, N.E. The vibration dance of the honey bee. I. Communication regulating foraging on two time scales. *Anim. Behav.* **1986**, *34*, 377–385. [[CrossRef](#)]
- Cristaldo, P.F.; Jandák, V.; Kutalová, K.; Rodrigues, V.B.; Brothánek, M.; Jiříček, O.; DeSouza, O.; Šobotník, J. The nature of alarm communication in *Constrictotermes cyphergaster* (Blattodea: Termitoidea: Termitidae): The integration of chemical and vibroacoustic signals. *Biol. Open* **2015**, *4*, 1649–1659. [[CrossRef](#)] [[PubMed](#)]
- Evans, T.A.; Lai, J.C.; Toledano, E.; McDowall, L.; Rakotonarivo, S.; Lenz, M. Termites assess wood size by using vibration signals. *Proc. Natl. Acad. Sci. USA* **2005**, *102*, 3732–3737. [[CrossRef](#)] [[PubMed](#)]
- Oberst, S.; Bann, G.; Lai, J.; Evans, T.A. Cryptic termites avoid predatory ants by eavesdropping on vibrational cues from their footsteps. *Ecol. Lett.* **2017**, *20*, 212–221. [[CrossRef](#)] [[PubMed](#)]
- Nunes, L.F.; Roxinol, J.A.; Cristaldo, P.F.; Marinho, R.; DeSouza, O. The use of tympanic arena as an alternative for behavioral vibroacoustic essays in termites (Blattodea: Isoptera). *Sociobiology* **2018**, *65*, 101–107. [[CrossRef](#)]
- Cunha, H.F.D.; Andrade Costa, D.; Espirito Santo Filho, K.D.; Silva, L.O.; Brandão, D. Relationship between *Constrictotermes Cyphergaster* Inquiline Termit. Cerrado (Isoptera: Termitidae). *Sociobiology* **2003**, *42*, 761–770.
- DeSouza, O.; Miramontes, O.; Santos, C.; Bernardo, D. Social facilitation affecting tolerance to poisoning in termites (Insecta, Isoptera). *Insectes Sociaux* **2001**, *48*, 21–24. [[CrossRef](#)]
- Šobotník, J.; Jirošová, A.; Hanus, R. Chemical warfare in termites. *J. Insect Physiol.* **2010**, *56*, 1012–1021. [[CrossRef](#)] [[PubMed](#)]
- Costa-Leonardo, A.M.; Haifig, I. Pheromones and exocrine glands in Isoptera. *Vitam. Horm.* **2010**, *83*, 521–549. [[PubMed](#)]



© 2019 by the authors. Licensee MDPI, Basel, Switzerland. This article is an open access article distributed under the terms and conditions of the Creative Commons Attribution (CC BY) license (<http://creativecommons.org/licenses/by/4.0/>).